Bounding the Higgs width at LHC

Edinburgh & Aachen, March, 2014

Keith Ellis, Fermilab

J.M.Campbell, R.K.Ellis and Ciaran Williams,
Gluon-Gluon Contributions to $W^+ W^-$ Production and Higgs Interference Effects,
arXiv:1107.5569
Bounding the Higgs width at the LHC using full analytic results for $gg \to e^- e^+ \mu^- \mu^+$,
arXiv:1311.3589
Bounding the Higgs width at the LHC: Complementary results from $H \to WW$,
arXiv:1312.1628

(see also, J.M.Campbell, R.K.Ellis, W. Giele and Ciaran Williams,
Finding the Higgs boson in decays to Zγ using the matrix element method at Next-to-Leading Order,
arXiv:1301.7086
J.M.Campbell, R.K.Ellis and Ciaran Williams,
Hadronic production of a Higgs boson and two jets at next-to-leading order,
arXiv:1001.4495.)

Higgs boson branching fractions

- Large number of observable SM Higgs decays
- We will consider WW*,ZZ*.
- ZZ* is 3%, before BR to observable mode.
- $\Gamma_H^{SM} \approx 4$ MeV.

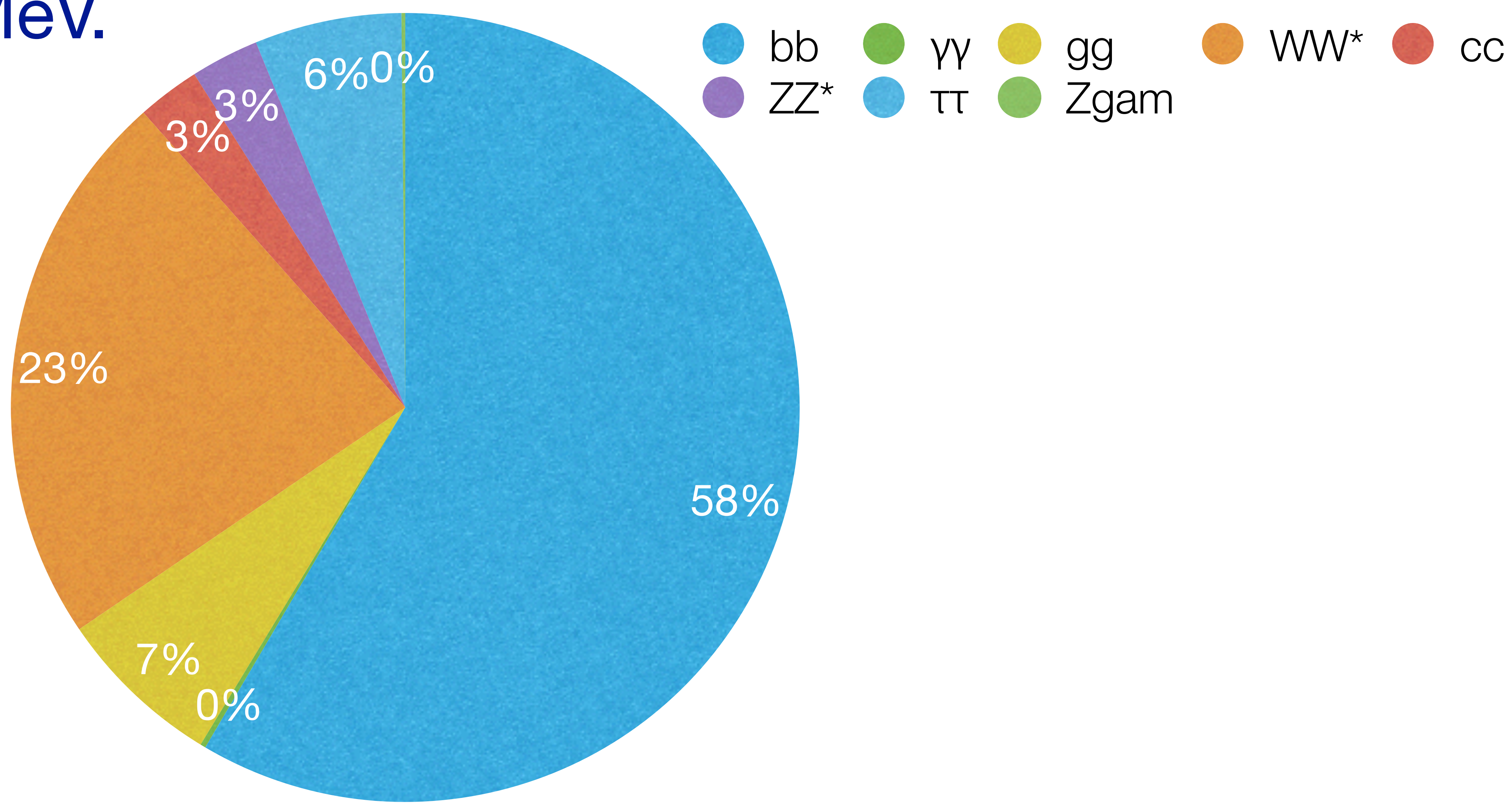

The lifetime (total width) of the Higgs boson

Particle	Width[MeV]	Lifetime[s]
t	$\sim 1,300$	$\sim 5 \times 10^{-25}$
W	$\sim 2,000$	$\sim 3 \times 10^{-25}$
Z	$\sim 2,500$	$\sim 2.6 \times 10^{-25}$
h	4.21 ± 0.16	$\sim 1.65 \times 10^{-22}$
b	4.4×10^{-10}	$\sim 1.5 \times 10^{-12}$

- Higgs boson lives longer than the t,W or Z, but not long enough to measure the lifetime directly.
- Width is very much less than experimental resolution ~1 GeV.
- Direct scan of the Higgs boson width will (only) be possible at a muon collider.

Narrow width approximation

* In the limit $\Gamma/M_h \rightarrow 0$ we may replace the Breit-Wigner distribution by a delta function.

$$\frac{1}{(\hat{s} - M_h^2)^2 + M_h^2 \Gamma_h^2} \approx \frac{\pi}{M_h \Gamma_h} \, \delta(\hat{s} - M_h^2) \; .$$

* For the standard model Higgs, Γ/M_h = 1/30,000 so narrow width approximation should apply.

Rescaling properties of the cross section on the peak

- In the narrow width approximation

$$\sigma(i \to H) \times BR(H \to X) = |M(i \to h)|^2 \frac{\Gamma(h \to X)}{\Gamma_h} \sim \frac{g_i^2 g_f^2}{\Gamma_h}$$

- Measurements on the Higgs peak, are only sensitive to the ratio, $\frac{g_i^2 g_f^2}{\Gamma_h}$

- Performing the rescaling leaves the measurement unchanged.

$$\begin{aligned} g_i &\to \xi g_i \\ g_f &\to \xi g_f \\ \Gamma_H &\to \xi^4 \Gamma_H \end{aligned}$$

Signal strength measurements

- Signal strength measurements, (that assume a value for the total width), confirm that $g_i^2 g_f^2/\Gamma_h$ is close to its standard model value.

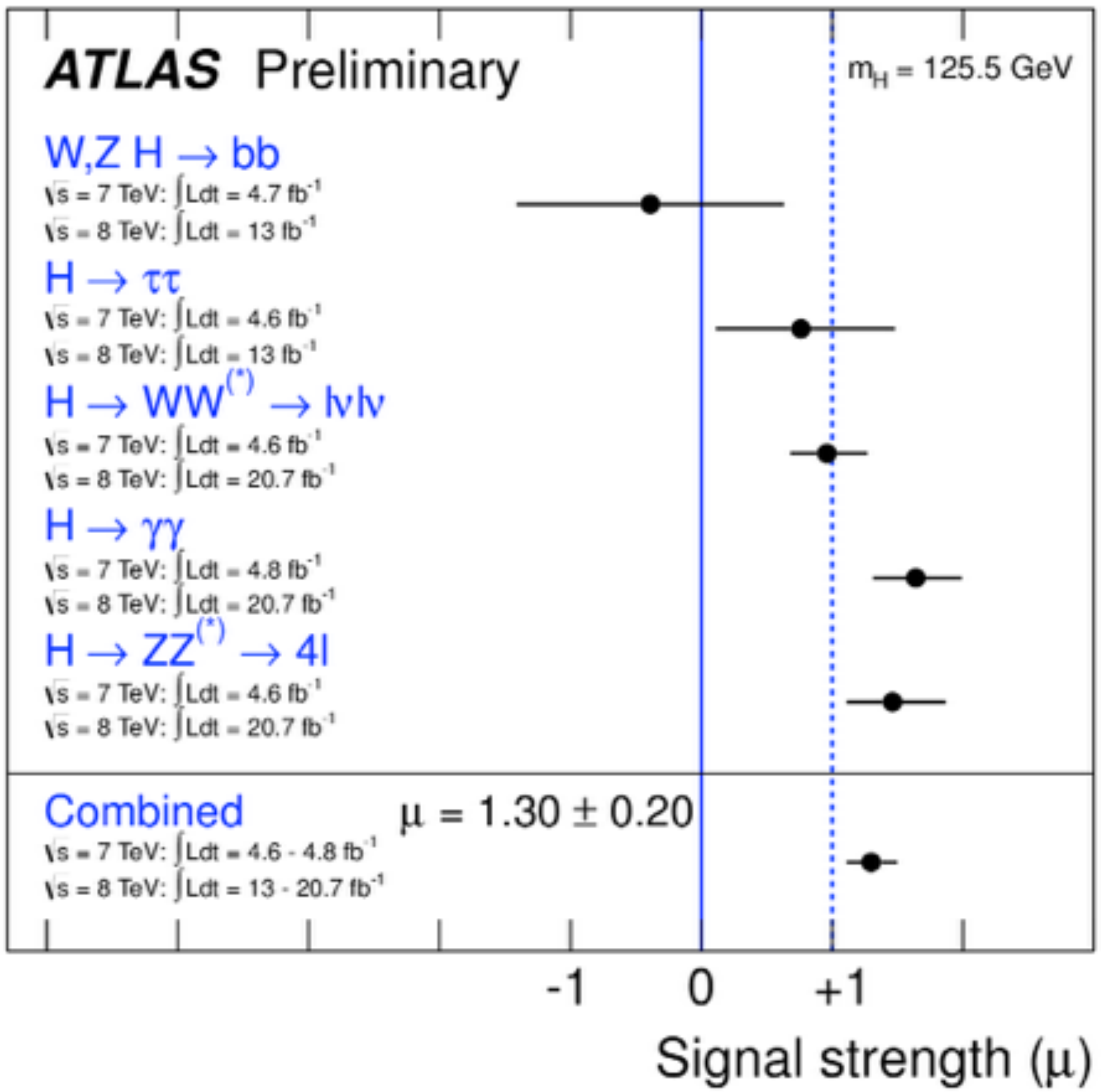

Basic process for this talk: $pp \rightarrow ZZ \rightarrow e^- e^+ \mu^- \mu^+$

$$p + p \rightarrow H \rightarrow ZZ$$

$$\hookrightarrow \mu^- + \mu^+$$

$$\hookrightarrow e^- + e^+ \,.$$

$$p + p \rightarrow Z/\gamma^* + Z/\gamma^*$$

$$\hookrightarrow \mu^- + \mu^+$$

$$\hookrightarrow e^- + e^+$$

- Consider the contributing Feynman diagrams.

Technically, only non-identical fermions although identical fermion effects are known to be small, except in the singly resonant region.

Narrow width approximation for Higgs boson

- How can it fail?
  - $\Gamma_H / M_H = 1/30{,}000$

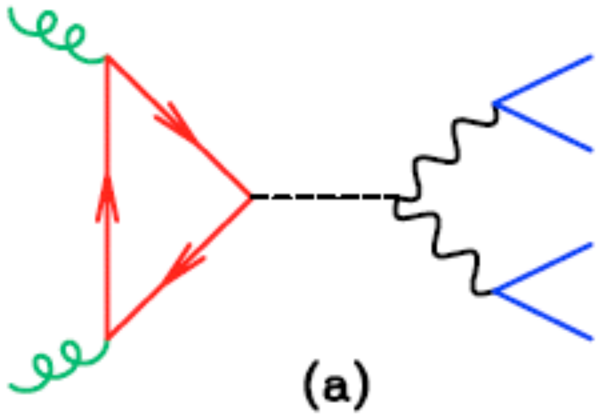

- It fails spectacularly for $gg \to H \to ZZ^{(*)} \to e^- e^+ \mu^- \mu^+$.

- At least 15% of the cross section comes from m_{4l}>130GeV.

  Kauer, Passarino,arXiv:1206.4803

- Similar tail for H→WW.

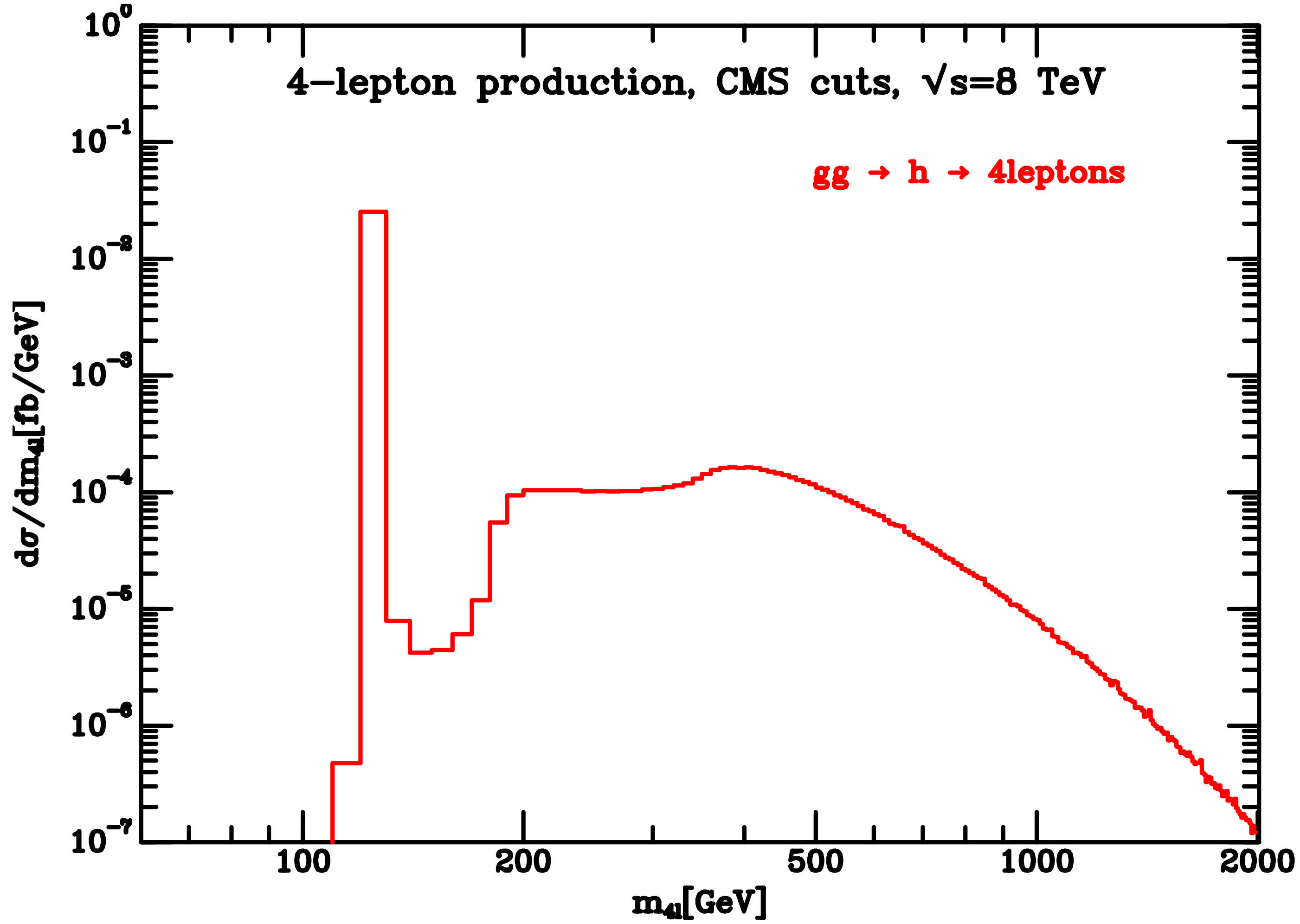

$pp \to e^- e^+ \mu^- \mu^+$ in the standard model

- Mishmash of orders in perturbation theory

$(a): g(-p_1) + g(-p_2) \to H \to e^-(p_3) + e^+(p_4) + \mu^-(p_5) + \mu^+(p_6)$	$O(g_s^2 e^4)$
$(b): q(-p_1) + g(-p_2) \to H \to e^-(p_3) + e^+(p_4) + \mu^-(p_5) + \mu^+(p_6) + q(p_7)$	$O(g_s^3 e^4)$
$(c): q(-p_1) + \bar{q}(-p_2) \to e^-(p_3) + e^+(p_4) + \mu^-(p_5) + \mu^+(p_6)$	$O(e^4)$
$(d): q(-p_1) + g(-p_2) \to e^-(p_3) + e^+(p_4) + \mu^-(p_5) + \mu^+(p_6) + q(p_7)$	$O(g_s e^4)$
$(e): g(-p_1) + g(-p_2) \to e^-(p_3) + e^+(p_4) + \mu^-(p_5) + \mu^+(p_6)$	$O(g_s^2 e^4)$

- Representative diagrams are:-
- (a) and (e), (b) and (d) can interfere.
- (b-d) interference does not overwhelm (a-e) see later.

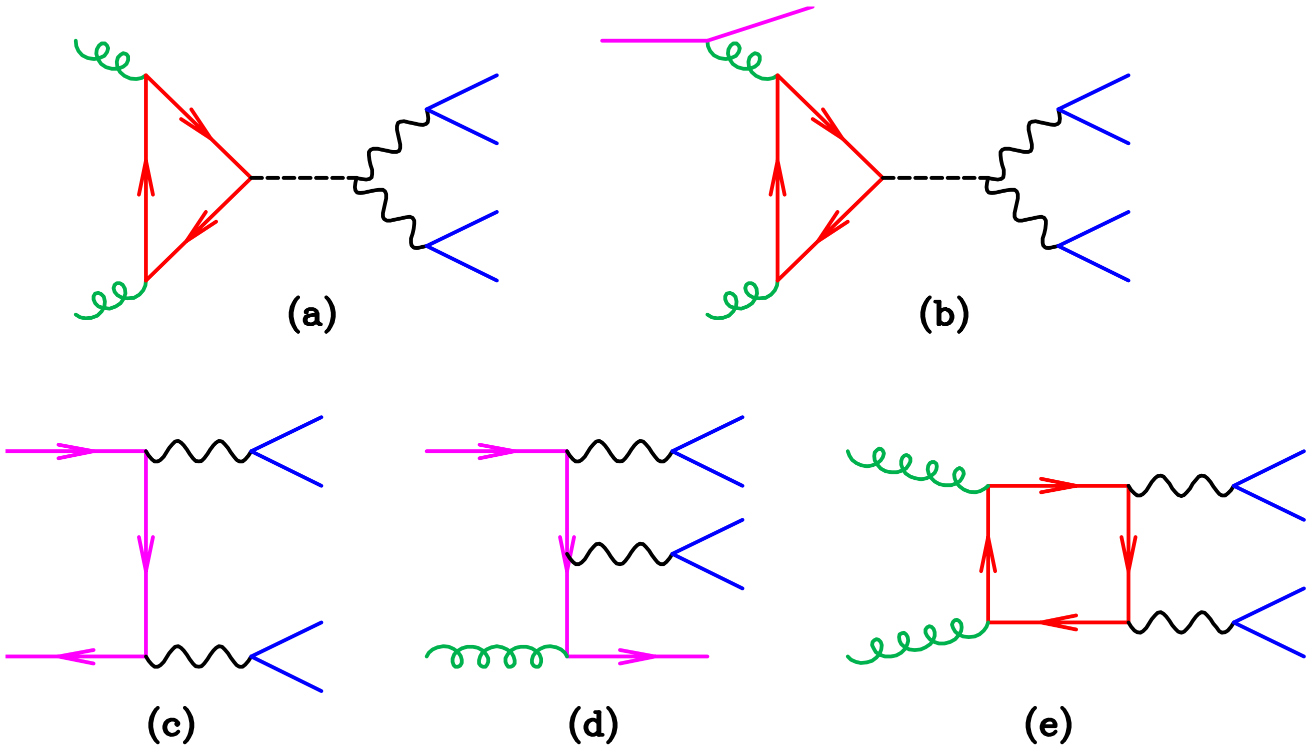

The big picture @ 8TeV

- Peak at Z mass due to singly resonant diagrams.
- Interference is an important effect.
- Destructive at large mass, as expected.
- With the standard model width, Γ_H , challenging to see enhancement/deficit due to Higgs channel.

$$p_{T,\mu} > 5 \text{ GeV}, \quad |\eta_\mu| < 2.4,$$
$$p_{T,e} > 7 \text{ GeV}, \quad |\eta_e| < 2.5,$$
$$m_{ll} > 4 \text{ GeV}, \quad m_{4\ell} > 100 \text{ GeV}.$$

CMS cuts
CMS PAS HIG-13-002

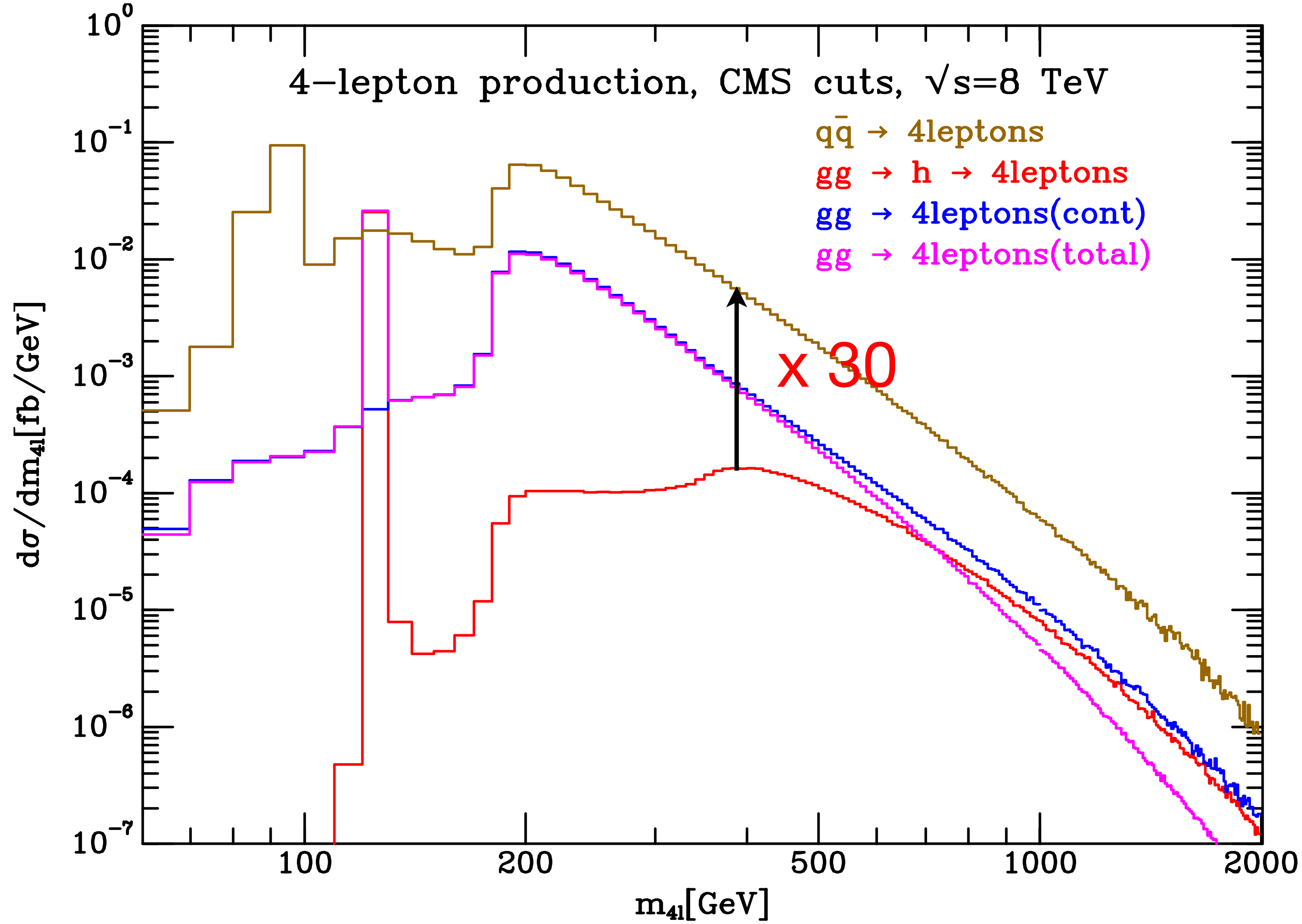

Higgs being Higgs

- Consider right hand side of gluon-gluon initiated diagrams.
- tt → ZZ, longitudinal modes of Z-bosons.

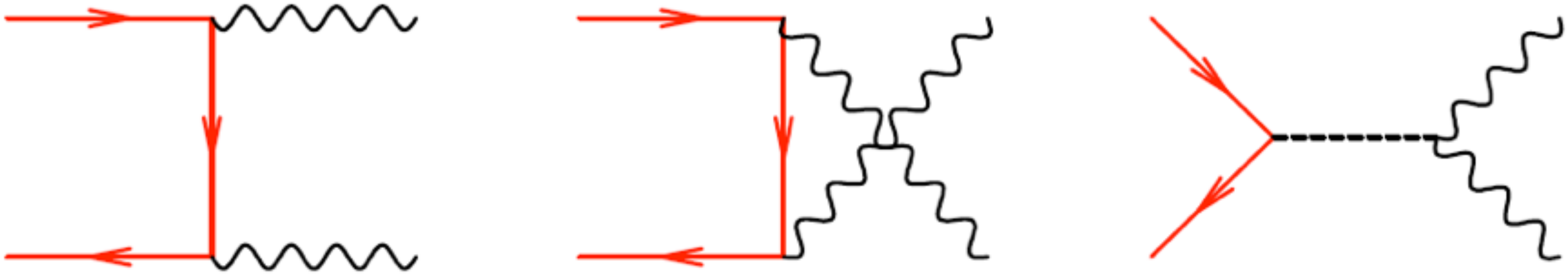

$a_2E^2+(b_1+a_1)m_tE$ $\quad$ $-a_2E^2+(c_1-a_1)m_tE$ $\quad$ $-(b_1+c_1)\, m_tE$

- Higgs tail has to be there to cancel bad high energy behavior of continuum diagrams.
- Observation of this cancellation, (if possible) is as interesting as longitudinal WW,ZZ scattering.

Caola-Melnikov method for Higgs width

- Higgs cross under the peak, section depends ratio of couplings and width.

$$\sigma_{\rm peak} \propto \frac{g_i^2 g_f^2}{\Gamma}$$

- Measurements at the peak cannot untangle couplings and width.

- Off-peak cross section is independent of the width, but still depends on $g_i^2 g_f^2$ (modulo interference, see later).

$$\sigma_{\rm off} \propto g_i^2 g_f^2$$

- Taking ratio

$$\frac{\left(\frac{\sigma_{\rm off}}{\sigma_{\rm peak}}\right)_{\rm experimental\ gg}}{\left(\frac{\sigma_{\rm off}}{\sigma_{\rm peak}}\right)_{\rm theoretical\ SM}} = \frac{\Gamma}{\Gamma^{\rm SM}}$$

- Ratio depends linearly on the Higgs boson width.

Caola-Melnikov method

* Although the interference has to be there, it is not essential for the CM method.
* Destructive interference actually weakens the bound that is obtained.
* CM method relies on accurate theoretical values for 4-charged lepton cross section (including the interference) both on and off-peak.

Diagrams for gg→Z/g*+Z/g*

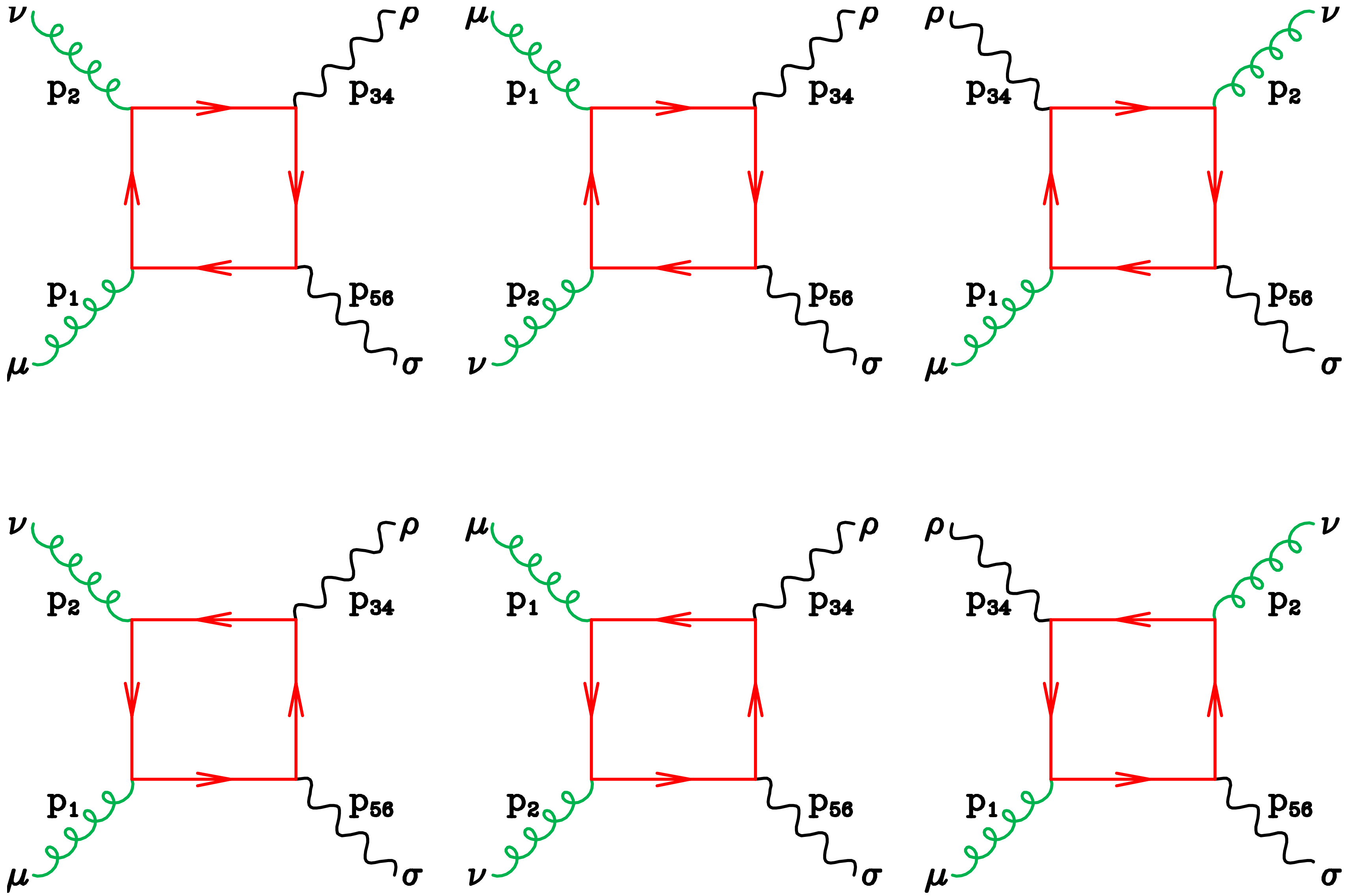

* Classify by the chirality of coupling to Z, i.e. LL, LR (and the related RR and RL).

History: $gg \to ZZ \to e^- e^+ \mu^- \mu^+$

- Calculation requires VV or AA piece or equivalently LL and LR piece.
- VV piece calculated in 1971, dispersive technique
  Constantini, de Tollis, Pistoni Nuovo Cim A2 1971
- (AA-VV) piece calculated for on-shell Z's, (inadequate for year>2012 purposes) Glover and van der Bij NPB321 (1989)
- Extension to off-shell Z's (no analytic formula for VV) Zecher et al, hep-ph/9404295
- gg2VV code, Kauer and Passarino, 1206.4803
- No published analytic form for the VV(LL) piece since 1971.
- Our aim: to obtain fast, stable code, to include in MCFM, using modern methods. Publish formula with value at a given phase space point, so it is feasible for other authors to implement. Campbell, Ellis, Williams 1311.3589

NLO revolution

- Dramatic advances in both analytic and numeric calculations, (including interplay between the two). Key ingredients
    - First modern use of unitarity for one-loop calculations (Bern,Dixon,Kosower)
    - Generalized unitarity for box diagrams(Britto, Cachazo, Feng)
    - OPP reduction, (Ossola, Papadopoulos, Pittau)
    - Melding of OPP with the Unitarity method (Ellis, Giele, Kunzst).
    - Development of techniques for both cut-constructible and rational parts, (OPP, Giele,Kunszt, Melnikov, Badger...)
    - Standard tabulation of all integrals (including divergent), (Ellis, Zanderighi)
    - Development of “Madgraph” style codes for NLO, (Gosam, aMC@NLO. ....).

Ingredients of a one-loop calculation

- Any one-loop amplitude expressible as a sum of box,triangle,bubble,tadpole scalar integrals+rational piece

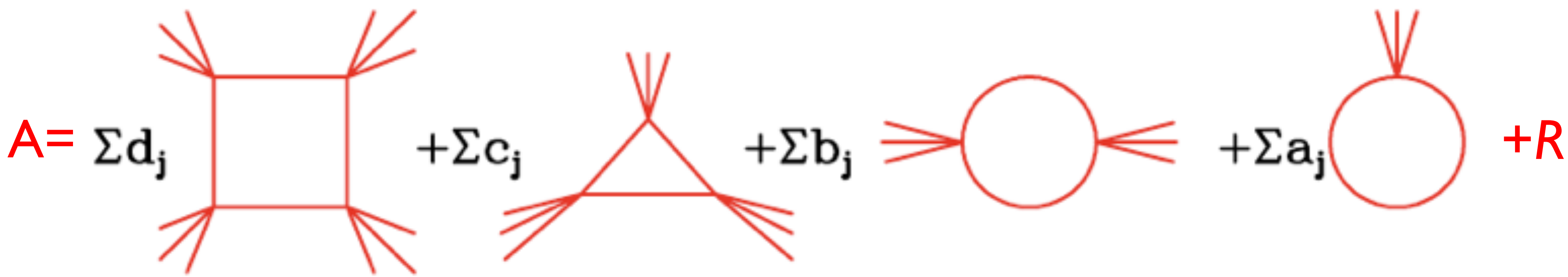

- Scalar integrals, finite and divergent are all known.
  - Scalar integral=loop integral with 1 in numerator
  - We use the ff and QCDLoop libraries, (see qcdloop.fnal.gov).
- *R* (rational part) is a finite vestige of the regularization procedure.
- Coefficients determined using analytic unitarity, (Bern-Dixon-Kosower, Britto,Cachazo,Feng,Forde,Badger....)

QCDLoop.fnal.gov

- RKE, Giulia Zanderighi, Loopfest 2008

General one-loop integral, finite or divergent as a Laurent series in ε

EZ Enterprises are proud to present:-

QCDLoop™

Never calculate a scalar one-loop integral ever again!

One stop shopping for all your one-loop needs!

Operators are standing by, call 1-800-QCDLoop today

"If you need one-loop, do yourself a favor, make it EZ"

Free shipping!

but wait, there's even more …

One loop diagrams

* We want to consider tensor integrals of the form, where d_i are propagator factors

$$I^{\mu_1 \ldots \mu_M} = \int \frac{d^D l}{i\pi^{D/2}} \frac{l^{\mu_1} \ldots l^{\mu_M}}{d_1 d_2 \ldots d_N}$$

* Passarino and Veltman wrote a form factor expansion for one loop integrals, e.g.

$$\int \frac{d^D l}{i\pi^{D/2}} \frac{l^\mu}{l^2 (l+p_1)^2 (l+p_1+p_2)^2} = C_1(p_1,p_2) p_1^\mu + C_2(p_1,p_2) p_2^\mu$$

* Contracting with p_1 and p_2 and using the identities

$$l \cdot p_1 = \tfrac{1}{2}[(l+p_1)^2 - l^2 - p_1^2], l \cdot p_2 = \tfrac{1}{2}[(l+p_1+p_2)^2 - (l+p_1)^2 - p_2^2 - 2p_1 \cdot p_2]$$

One loop diagrams (continued)

- We derive a linear equation expressing C_1, C_2 as scalar integrals

$$\begin{pmatrix} 2p_1 \cdot p_1 & 2p_1 \cdot p_2 \\ 2p_2 \cdot p_1 & 2p_2 \cdot p_2 \end{pmatrix} \begin{pmatrix} C_1 \\ C_2 \end{pmatrix} = \begin{pmatrix} R_1 \\ R_2 \end{pmatrix}$$

$$R_1 = [B_0(p_1+p_2) - B_0(p_2) - p_1^2\, C_0(p_1,p_2)]$$
$$R_2 = [B_0(p_1) - B_0(p_1+p_2) - (p_2^2 + 2p_1 \cdot p_2)\, C_0(p_1,p_2)]$$

$$C_0(p_1,p_2) = \int [dl] \frac{1}{l^2(l+p_1)^2(l+p_1+p_2)^2}, \; B_0(p_1) = \int [dl] \frac{1}{l^2(l+p_1)^2}$$

- Solution involves the inverse of the Gram matrix $G_{ij} \equiv 2p_i \cdot p_j$

$$G^{-1} = \begin{pmatrix} +p_2 \cdot p_2 & -p_1 \cdot p_2 \\ -p_1 \cdot p_2 & +p_1 \cdot p_1 \end{pmatrix} /[2(p_1 \cdot p_1\, p_2 \cdot p_2 - (p_1 \cdot p_2)^2)]$$

- Apparent singularity as when p_1 parallel to p_2 cancels because of relationships between integrals in this limit.

One loop amplitudes

- General strategy: One loop amplitude expressed in terms of scalar box, triangle, bubble integrals + rational part

$$A = \sum_{j=1}^{3} d_j(1^{h_1}, 2^{h_2})\, D_0(j) + \sum_{j=1}^{6} c_j(1^{h_1}, 2^{h_2})\, C_0(j) + \sum_{j=1}^{6} b_j(1^{h_1}, 2^{h_2})\, B_0(j) + R(1^{h_1}, 2^{h_2})$$

- As a general rule this reduction generates inverse Gram determinants giving apparent singularities.
- In our case

$$\begin{aligned}\Delta(p_1, p_2, p_{34}) &= \frac{1}{2} p_1 \cdot p_2 [4 p_1 \cdot p_{34}\, p_2 \cdot p_{34} - 2 p_1 \cdot p_2\, p_{34} \cdot p_{34}] \\ &= \frac{1}{2} p_1 \cdot p_2\, \langle p_1 | (p_3 + p_4) | p_2]\, [p_2 | (p_3 + p_4) | p_1 \rangle \\ &= (p_1 \cdot p_2)^2\, p_T^2\end{aligned}$$

- Apparent singularities at p_T=0 are particularly trying in this case,since cuts are placed on the p_T of the leptons not of the Z.

Diagrams for gg→Z/g*+Z/g*

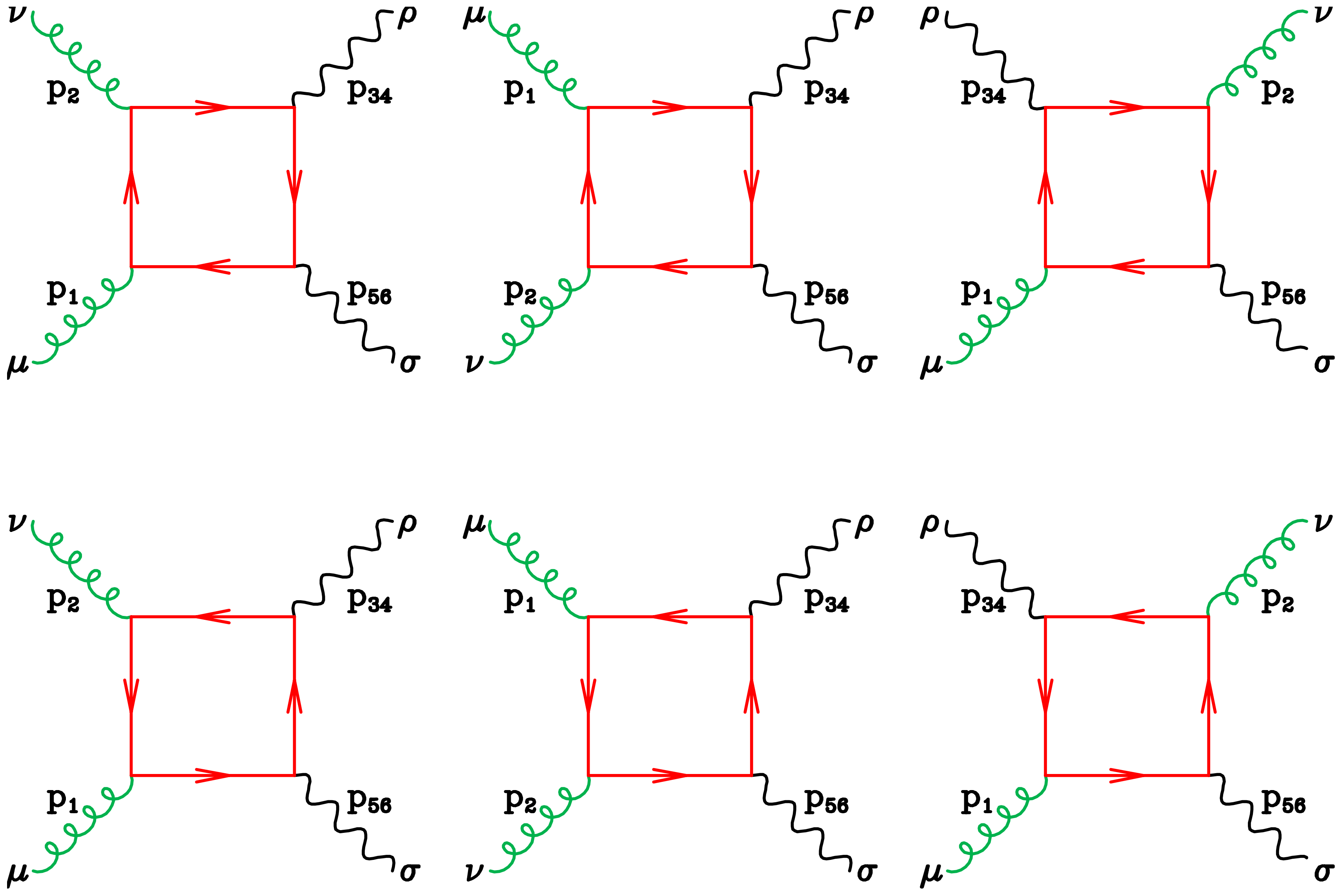

- Classify by the chirality of coupling to Z, i.e. LL, LR (and the related RR and RL).

LR piece (easy!)

- Hard to improve on the 1989 treatment of Glover-van der Bij, apart from extension to $p_{34}^2 \neq p_{56}^2$
- Vanishes for m→0.
- Tensor satisfying QCD gauge invariance, (indices μ and ν)

$$
\begin{aligned}
P_{LR}^{\mu\nu\rho\sigma} &= A_1 g^{\rho\sigma}\Big(g^{\mu\nu} - \frac{p_1^\nu p_2^\mu}{p_1\cdot p_2}\Big) \\
&+ A_2 g^{\rho\sigma}\Big(g^{\mu\nu} + \frac{2}{p_T^2}p_{34}^\mu p_{34}^\nu + \frac{p_{34}^2}{p_T^2 p_1\cdot p_2}p_1^\nu p_2^\mu - \frac{2p_1\cdot p_{34}}{p_T^2 p_1\cdot p_2}p_2^\mu p_{34}^\nu - \frac{2p_2\cdot p_{34}}{p_T^2 p_1\cdot p_2}p_1^\nu p_{34}^\mu\Big) \\
&+ A_3\Big(g^{\mu\sigma}g^{\nu\rho} + \frac{g^{\mu\nu}p_1^\sigma p_2^\rho}{p_1\cdot p_2} - \frac{g^{\nu\rho}p_1^\sigma p_2^\mu}{p_1\cdot p_2} - \frac{g^{\mu\sigma}p_1^\nu p_2^\rho}{p_1\cdot p_2}\Big) \\
&+ A_4\Big(g^{\mu\rho}g^{\nu\sigma} + \frac{g^{\mu\nu}p_1^\rho p_2^\sigma}{p_1\cdot p_2} - \frac{g^{\nu\sigma}p_1^\rho p_2^\mu}{p_1\cdot p_2} - \frac{g^{\mu\rho}p_1^\nu p_2^\sigma}{p_1\cdot p_2}\Big) \\
&+ A_5\frac{1}{p_1\cdot p_2}\Big(g^{\mu\sigma}p_1^\rho p_{34}^\sigma - g^{\mu\rho}p_1^\sigma p_{34}^\nu + g^{\nu\sigma}p_2^\rho p_{34}^\mu - g^{\nu\rho}p_2^\sigma p_{34}^\mu \\
&+ \frac{p_2\cdot p_{34}}{p_1\cdot p_2}g^{\mu\rho}p_1^\nu p_1^\sigma - \frac{p_2\cdot p_{34}}{p_1\cdot p_2}g^{\mu\sigma}p_1^\nu p_1^\rho + \frac{p_1\cdot p_{34}}{p_1\cdot p_2}g^{\nu\rho}p_2^\mu p_2^\sigma - \frac{p_1\cdot p_{34}}{p_1\cdot p_2}g^{\nu\sigma}p_2^\mu p_2^\rho\Big) \\
&+ A_6\frac{1}{p_1\cdot p_2}\Big(g^{\mu\sigma}p_1^\rho p_{34}^\nu - g^{\mu\rho}p_1^\sigma p_{34}^\nu + g^{\mu\rho}p_1^\nu p_1^\sigma\frac{p_2\cdot p_{34}}{p_1\cdot p_2} - g^{\mu\sigma}p_1^\nu p_1^\rho\frac{p_2\cdot p_{34}}{p_1\cdot p_2}\Big)
\end{aligned}
$$

Form factors for LR

- Form factors expressed in terms of Scalar Integrals C_0, D_0 and six-dimensional box integrals.

The six form factors A_i are given by, $(Y = s_{12} p_T^2 = 4 p_{34}.p_1 p_{34}.p_2 - s_{12} s_{34})$

$$
\begin{aligned}
A_1 &= \frac{m^2}{2 s_{12}} \Big[2\bar{s}_{134} C_0(3) + 2\bar{s}_{234} C_0(4) + 2\bar{s}_{156} C_0(5) + 2\bar{s}_{256} C_0(6) \\
&- 2Y D_0(1) + s_{12}(s_{12} - 4m^2)(D_0(1) + D_0(2) + D_0(3)) \Big] \\
A_2 &= 2m^2 \Big[D_0^{d=6}(3) + D_0^{d=6}(2) + C_0(2) + m^2 \Big(D_0(3) + D_0(2) - D_0(1) \\
A_3 &= \frac{1}{2} m^2 s_{12} \Big[D_0(3) - D_0(2) - D_0(1) \Big] \\
A_4 &= \frac{1}{2} m^2 s_{12} \Big[D_0(2) - D_0(3) - D_0(1) \Big] \\
A_5 &= \frac{m^2 s}{2 s_{234} s_{134}} \Big[2 s_{134} D_0^{d=6}(3) + 2 s_{234} D_0^{d=6}(2) - s_{234} s_{134} D_0(1) \\
&+ 4m^2 \Big(s_{134} D_0(3) + s_{234} D_0(2) \Big) + 2(s_{234} + s_{134}) C_0(2) \Big] \\
A_6 &= -\frac{m^2 s_{12}}{Y} \Big[\bar{s}_{134} C_0(3) - \bar{s}_{234} C_0(4) + \bar{s}_{156} C_0(5) - \bar{s}_{256} C_0(6) \Big] \equiv 0
\end{aligned}
$$

- Six-dimensional box (sum of 4-dim boxes and triangles) collects factors of Y or $(1/p_T^2)$

$$
\begin{aligned}
D_0^{d=6}(2) &= \frac{s_{134}}{2Y} \Big[\bar{s}_{134} C_0(3) + \bar{s}_{256} C_0(6) + s_{12} C_0(1) \\
&+ \Big(s_{12} - s_{34} - s_{56} + 2 \frac{s_{34} s_{56}}{s_{134}} \Big) C_0(2) - \Big(s_{12} s_{134} + \frac{4m^2 Y}{s_{134}} \Big) D_0(2) \Big]
\end{aligned}
$$

Expression for LL pieces (harder!)

- (Slight) generalization of integral basis to aid with numerical stability

$$A = \sum_{j=2}^{3} d_j(1^{h_1}, 2^{h_2})\, D_0^{d=6}(j) + \sum_{j=1}^{3} d_j(1^{h_1}, 2^{h_2})\, D_0(j)$$
$$+ \sum_{j=1}^{6} c_j(1^{h_1}, 2^{h_2})\, C_0(j) + \sum_{j=1}^{6} b_j(1^{h_1}, 2^{h_2})\, B_0(j) + R(1^{h_1}, 2^{h_2})$$

- Complete analytic forms for integral coefficients in terms of spinor products, e.g.

$$d_2^{d=6}(1^-, 2^+) = \frac{-1}{[3\,4]\langle 5\,6\rangle s_{134}} \frac{\langle 1|(3+4)|2]}{\langle 2|(3+4)|1]^3} \Big[\langle 2|(1+3)|4]^2 \langle 5|(3+4)|1]^2 + s_{134}^2 \langle 2\,5\rangle^2 [1\,4]^2\Big]$$

- Relatively simple formulae for each presented in paper.

$P_T=0$

- Translating back to Bjorken-Drell notation,

$$\langle 2|(3+4)|1] = \bar{u}_+(p_1)(\not{p}_3+\not{p}_4)v_+(p_2)$$

- Singular when 3+4 is a linear combination of 1 and 2.
- Pernicious in this case, because we cut of p_T's of leptons, not $p_T(Z)=p_3+p_4$,
- The singularity is only apparent, but it can cause numerical problems.
- Clear improvement when moving to new d=6 basis.

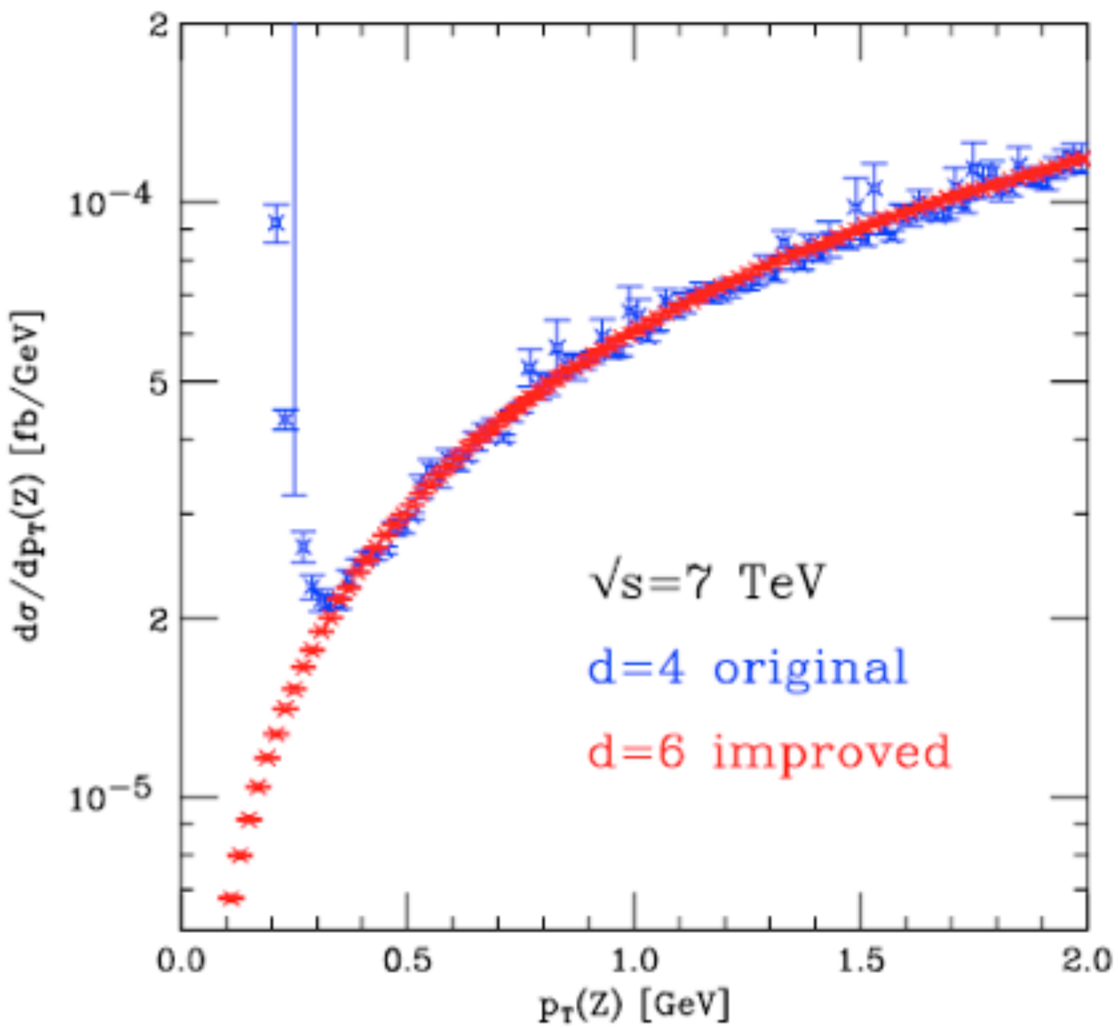

Why not just cut out the low p_T region?

- 8% of the $gg \to H \to ZZ^* \to e^- e^+ \mu^- \mu^+$ cross section, comes from the region where $p_T^Z < 7$GeV.
- We impose a cut of $p_T^Z < 0.1$GeV, (i.e. less than 0.01% of cross section.

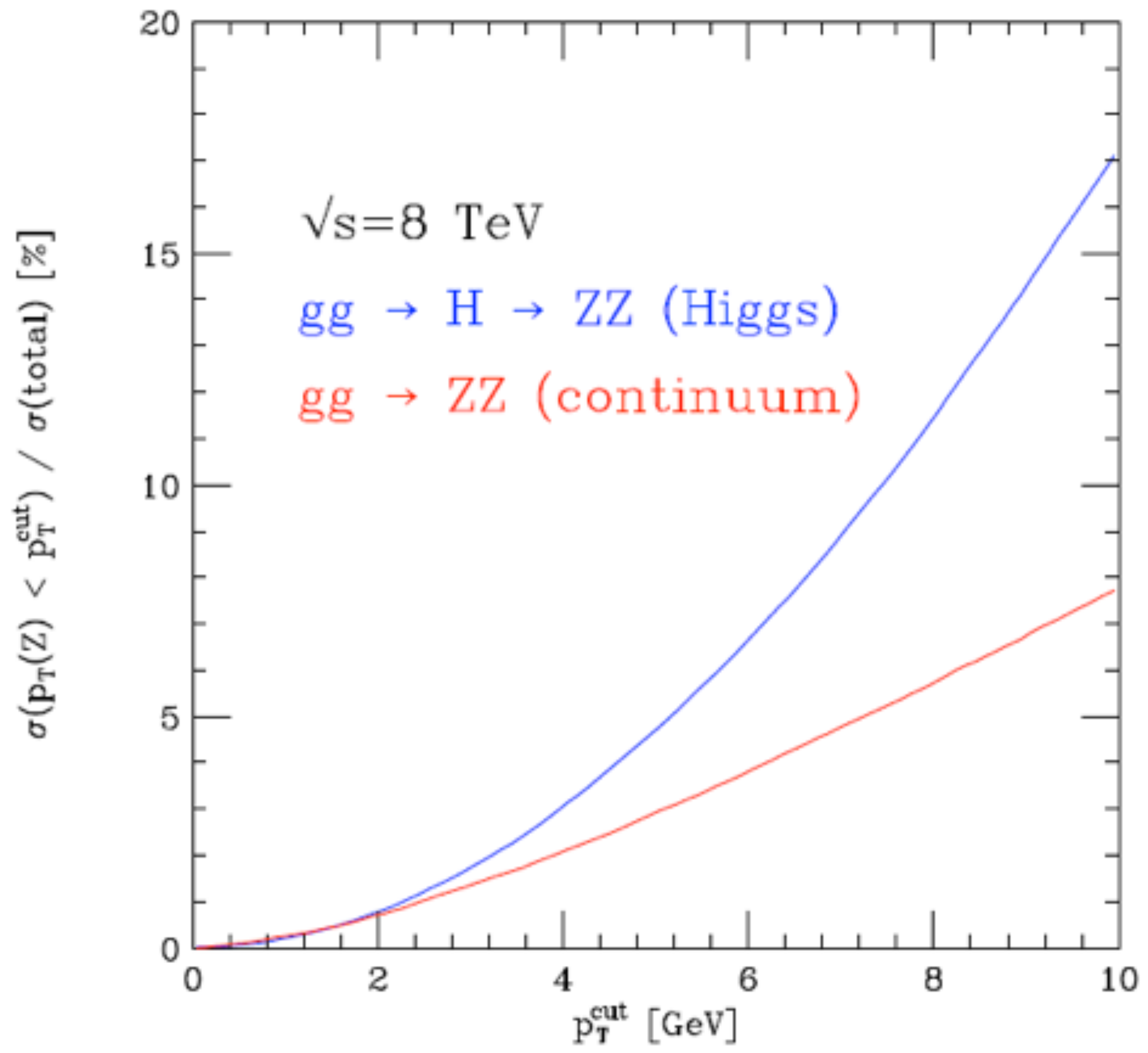

Size of interference @ 8 TeV

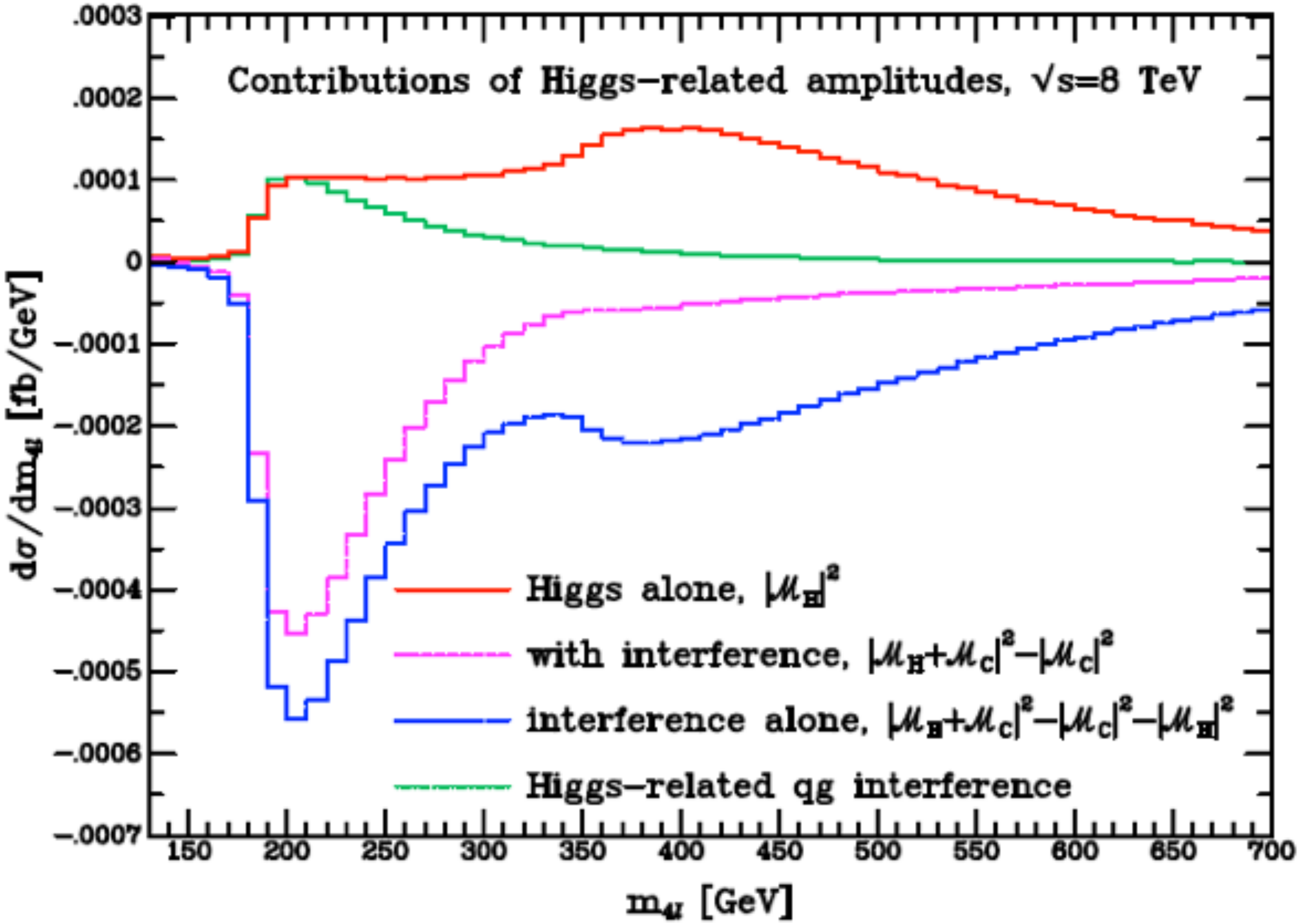

- Impossible to predict correct rate without correct accounting for interference.
- Higgs-related qg interference is not so big, especially above m4l>300GeV

Big picture @ 13 TeV

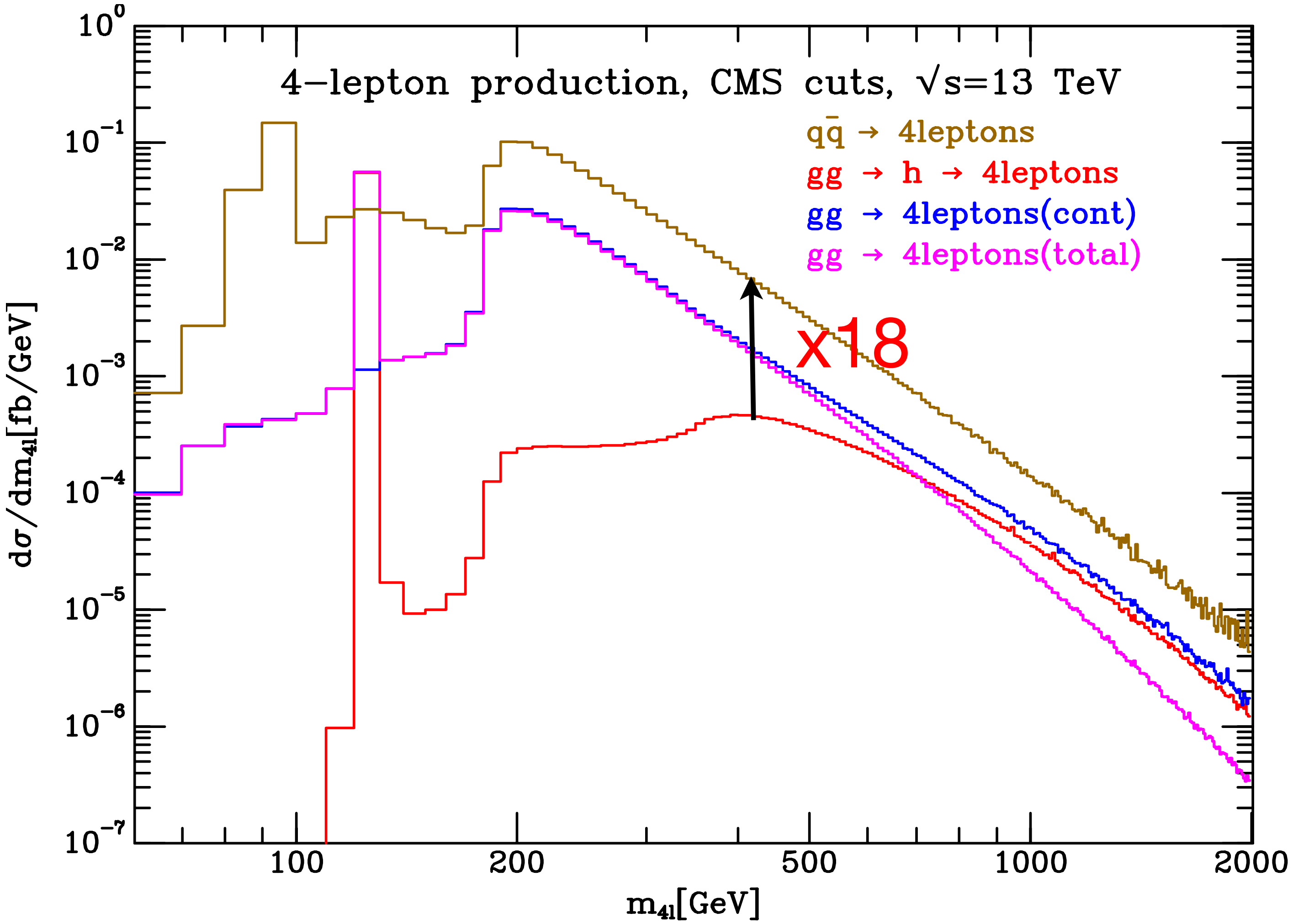

- σ_{qqb} (m_{4l}=400)/σ^{H}_{gg} (m_{4l}=400) ≈ 18 at $\sqrt{s}$=13 TeV
- (c.f. ~30 at $\sqrt{s}$=8 TeV).
- Measurement should improve at higher energy.

Quantifying the interference-comparison with CM

- Our results for interference differ (slightly) from CM paper.
- We believe that the reason is that CM used the double precision version of the Kauer code gg2VV, that contains a cut at p_T<7GeV, for continuum related pieces.

Energy	σ^H_{peak}	$\sigma^H_{off}(m_{4l} > 130\text{ GeV})$	$\sigma^{int}_{off}(m_{4l} > 130\text{ GeV})$
7 TeV	0.203	0.044	-0.086
8 TeV	0.255	0.061	-0.118

Energy	σ^H_{peak}	$\sigma^H_{off}(m_{4l} > 300\text{ GeV})$	$\sigma^{int}_{off}(m_{4l} > 300\text{ GeV})$
7 TeV	0.203	0.034	-0.050
8 TeV	0.255	0.049	-0.071

Quantifying the interference (pdf dependence).

* Choosing scale=$M_H/2$
* Cross sections in fb
* ~10% dependence on parton (gluon) distribution, in ratio, shown in orange.

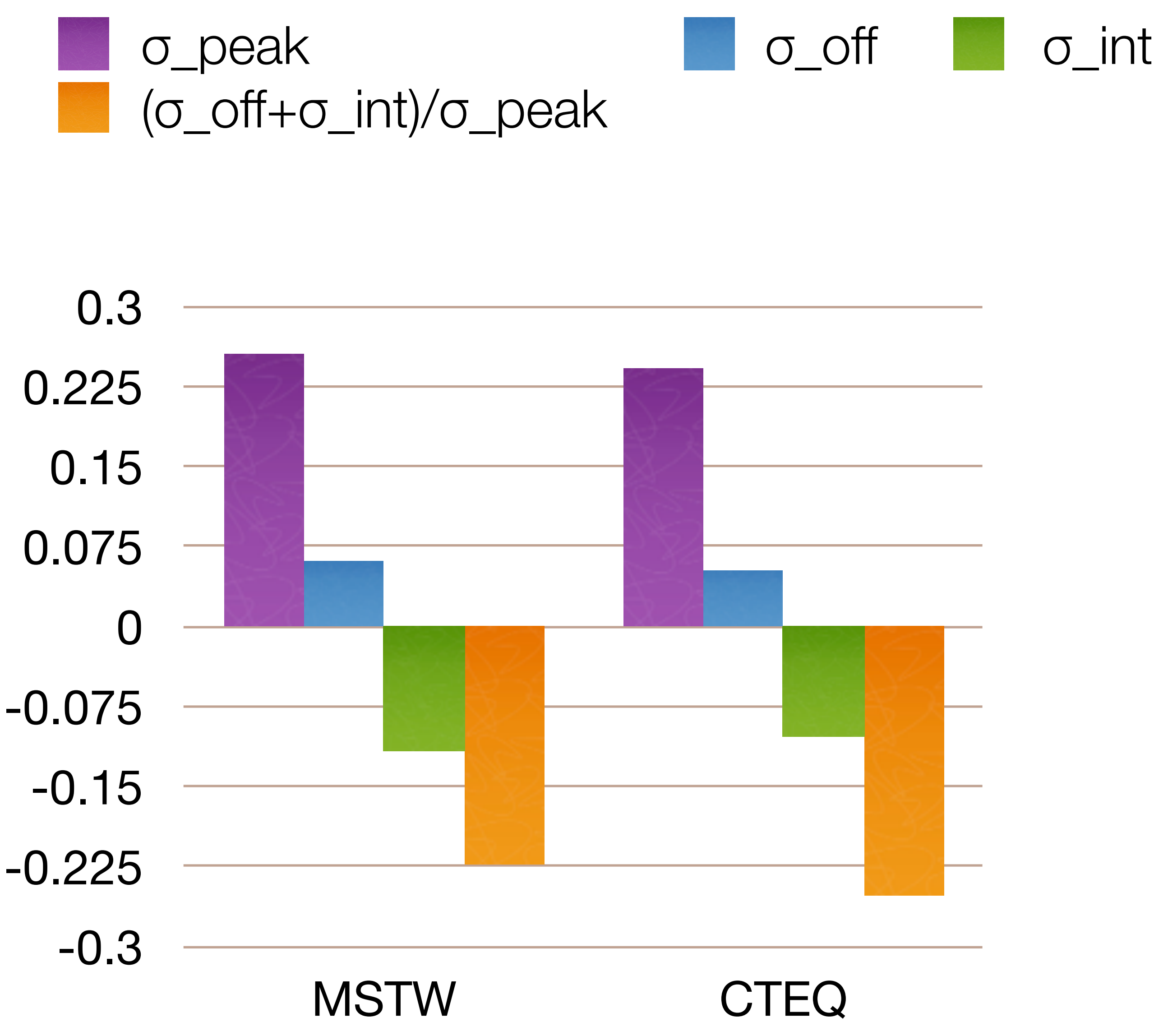

Quantifying the interference-scale dependence.

- Choosing scales, $m_H/2$ and more natural scale $m_{4l}/2$
- Large dependence on choice of scale ~50%, in off-peak/on-peak ratio (shown in orange)
- Adopt scale $m_{4l}/2$ for best prediction.

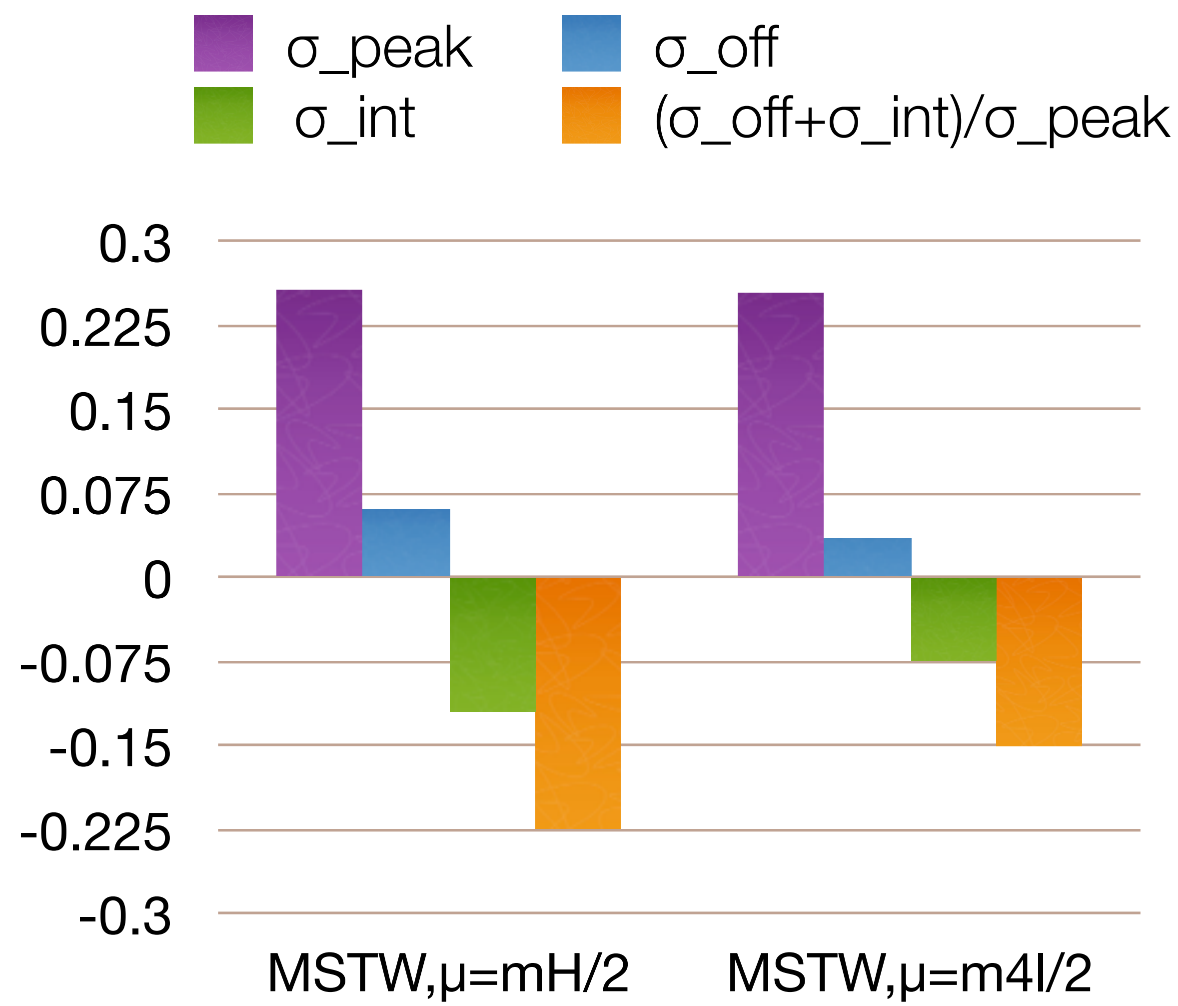

Best prediction
CMS cuts

Energy	pdf	σ^H_{peak}	$m_{4l} > 130$ GeV σ^H_{off}	$m_{4l} > 130$ GeV σ^{int}_{off}	$m_{4l} > 300$ GeV σ^H_{off}	$m_{4l} > 300$ GeV σ^{int}_{off}
7 TeV	MSTW	0.203	0.025	-0.053	0.017	-0.025
	CTEQ	0.192	0.021	-0.047	0.015	-0.021
8 TeV	MSTW	0.255	0.034	-0.073	0.025	-0.036
	CTEQ	0.243	0.031	-0.065	0.022	-0.031
13 TeV	MSTW	0.554	0.108	-0.215	0.085	-0.122
	CTEQ	0.530	0.100	-0.199	0.077	-0.111

Rough and ready estimate of current bound on Γ_H

* Update of Caola-Melnikov analysis, using our best prediction.
* Using the results from our best prediction we find for $\sigma_{off} \equiv \sigma^H_{off} + \sigma^{int}_{off}$ at 8TeV.

$$\sigma_{off}(m_{4\ell} > 130 \text{ GeV}) = 0.034\left(\frac{\Gamma_H}{\Gamma_H^{SM}}\right) - 0.073\sqrt{\frac{\Gamma_H}{\Gamma_H^{SM}}}$$

$$\sigma_{off}(m_{4\ell} > 300 \text{ GeV}) = 0.025\left(\frac{\Gamma_H}{\Gamma_H^{SM}}\right) - 0.036\sqrt{\frac{\Gamma_H}{\Gamma_H^{SM}}}$$

* Therefore normalizing to the number of events observed at the peak we can estimate number of Higgs-related events off-peak (appropriately weighting to combine 7 and 8 TeV data).

$$N^{4\ell}_{off}(m_{4\ell} > 130 \text{ GeV}) = 2.78\left(\frac{\Gamma_H}{\Gamma_H^{SM}}\right) - 5.95\sqrt{\frac{\Gamma_H}{\Gamma_H^{SM}}}$$

$$N^{4\ell}_{off}(m_{4\ell} > 300 \text{ GeV}) = 2.02\left(\frac{\Gamma_H}{\Gamma_H^{SM}}\right) - 2.91\sqrt{\frac{\Gamma_H}{\Gamma_H^{SM}}}$$

Updated limit on Higgs width

- Use the number of events observed in the off-peak region (451) and number expected on the basis of continuum alone (431±31)

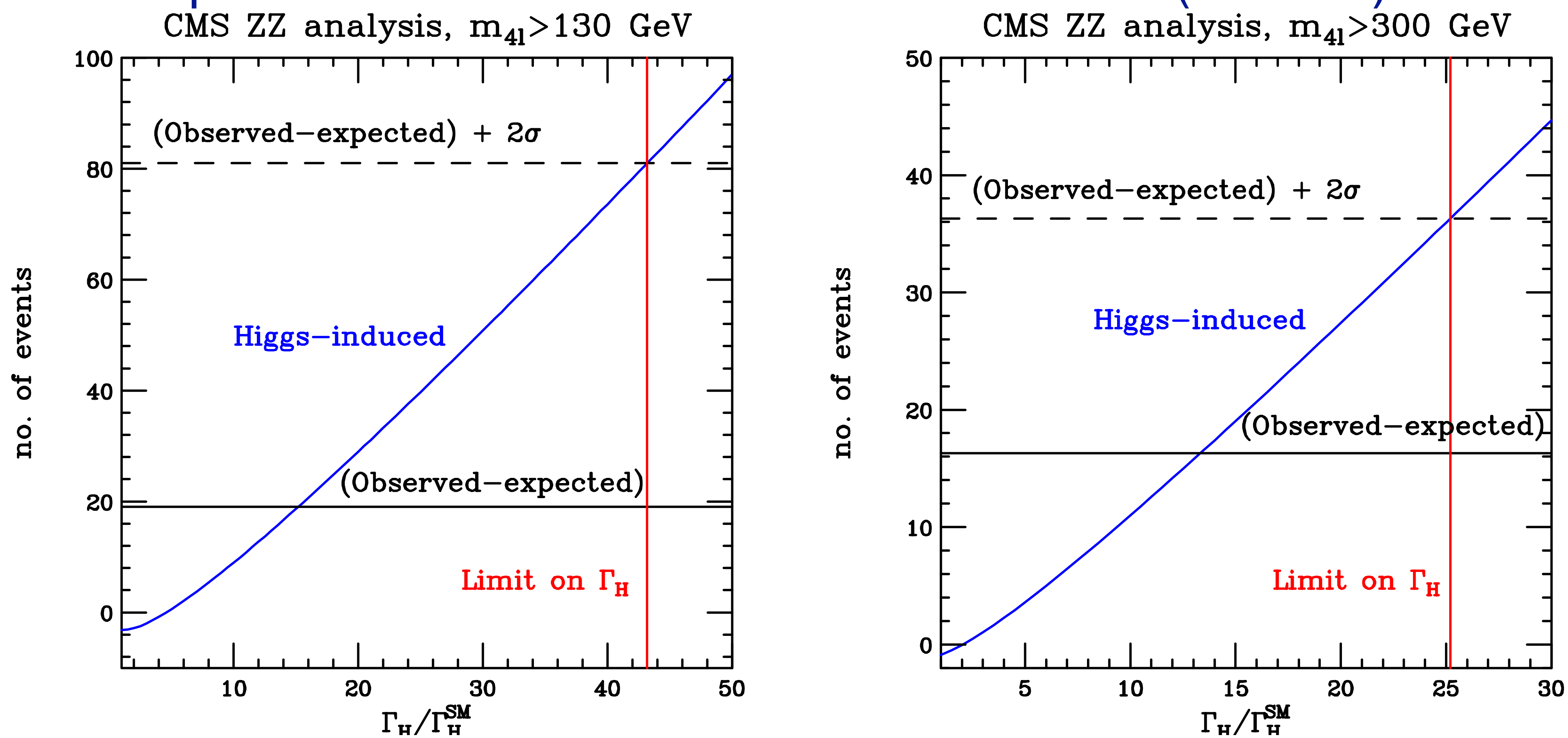

$$\Gamma_H < 43.2\,\Gamma_H^{SM} \text{ at } 95\% \text{ c.l.,} \quad (m_{4\ell} > 130 \text{ GeV analysis})$$
$$\Gamma_H < 25.2\,\Gamma_H^{SM} \text{ at } 95\% \text{ c.l.,} \quad (m_{4\ell} > 300 \text{ GeV analysis})$$

- This analysis is indicative only and needs to be repeated by the experiments.

Improvement by matrix element method

* Associate a probabilistic weight to each input event.

$$P_{LO}(\phi) = \frac{1}{\sigma_{LO}} \sum_{i,j} \int dx_1 dx_2\, \delta(x_1 x_2 s - Q^2) f_i(x_1) f_j(x_2) \hat{\sigma}_{ij}(x_1, x_2, \phi)$$

$P_{q\bar{q}}$: $q\bar{q}$ initiated background.

P_{gg} : gg initiated pieces, including Higgs signal, box diagrams and interference.

P_H : gg initiated Higgs signal squared.

$$D_S = \log\left(\frac{P_H}{P_{gg} + P_{q\bar{q}}}\right)$$

* Test of discriminant on different components.

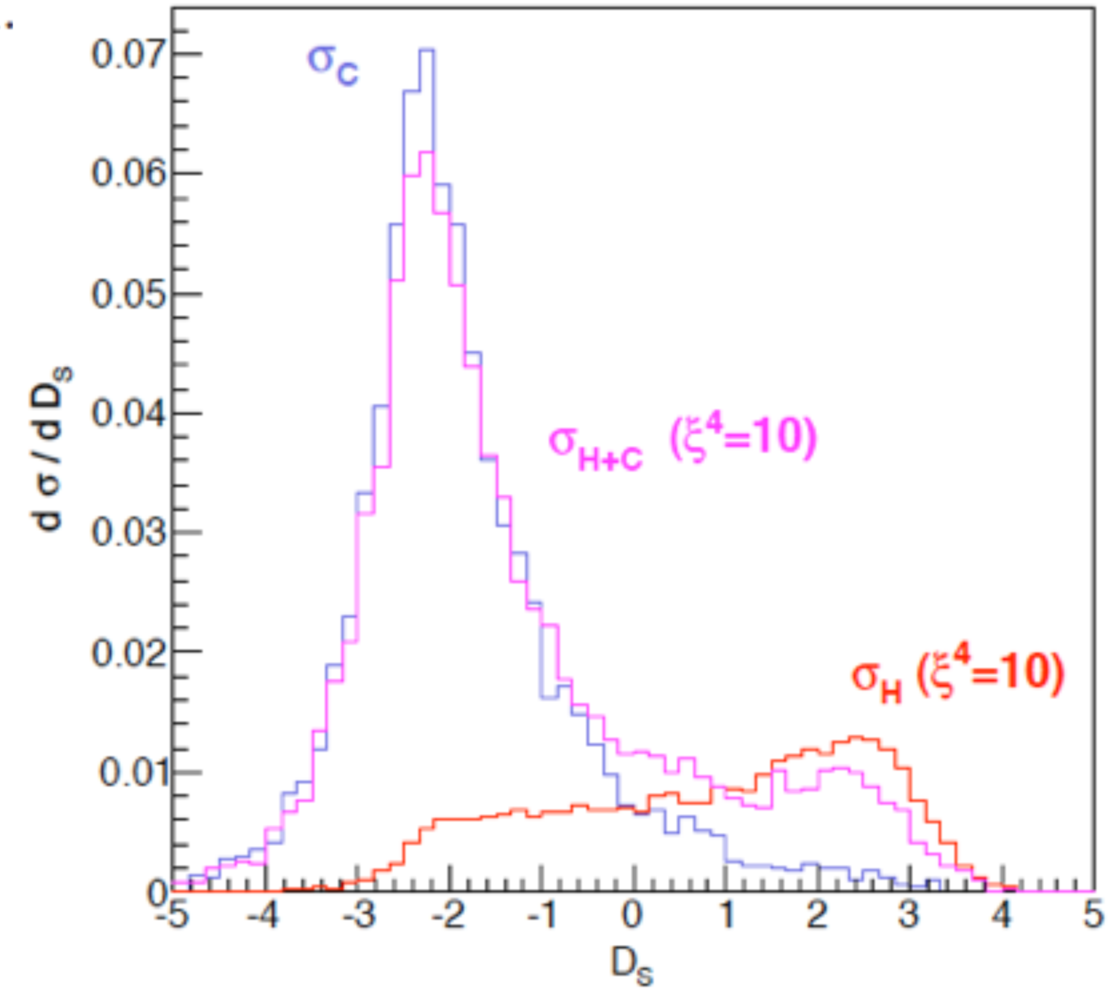

Application to Monte Carlo pseudo-data

- Rescale Monte Carlo to give 400 N_{qq} events.
- Attempt to choose statistical errors to match CMS analysis.
- Without using discriminant, we obtain limits in line with cut and count analysis.
- Cutting at D_s=1 we obtain
- Limit is 1.6 times better than result for m_{4l}>300GeV cut.
- To be repeated by experiment!

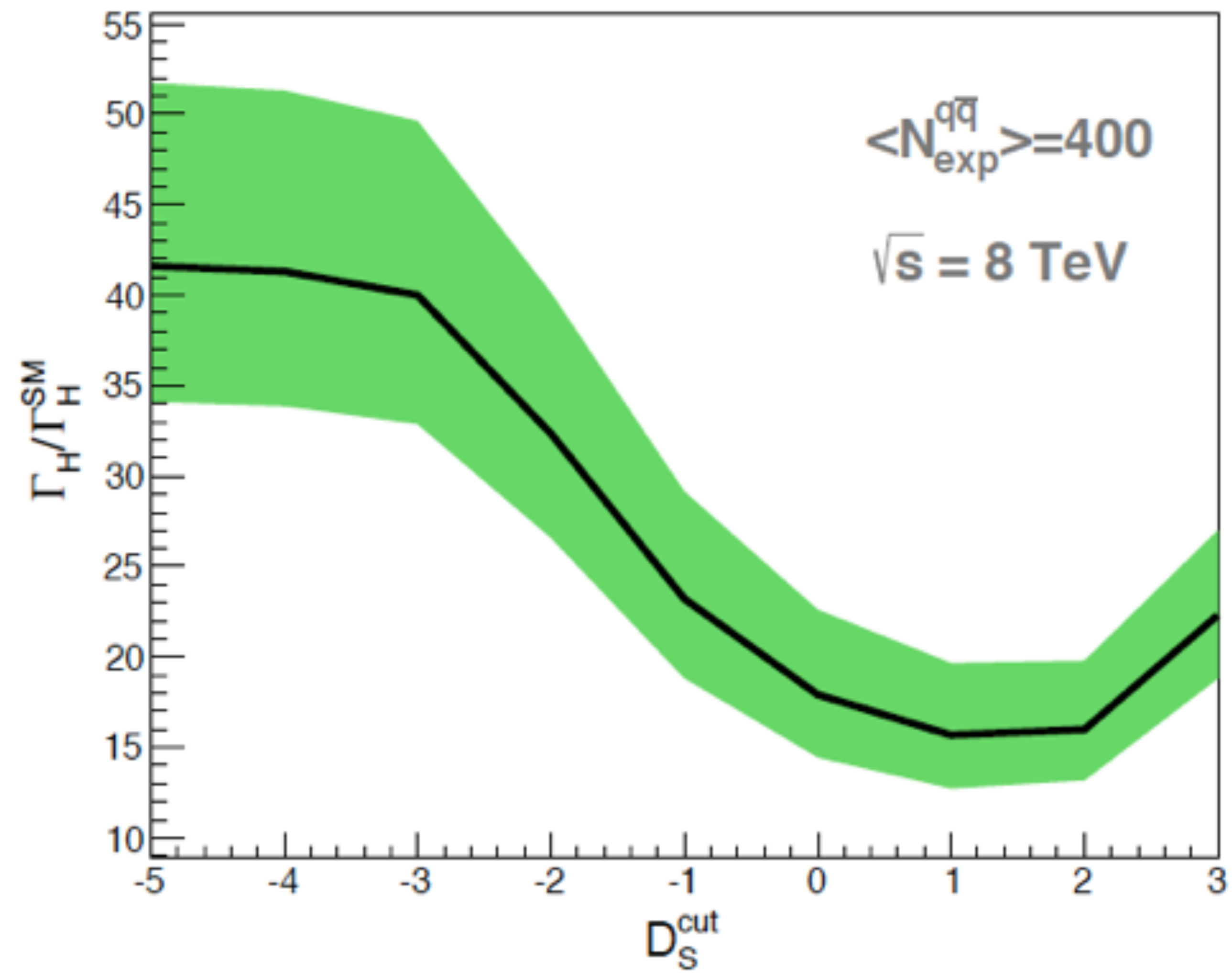

$$\Gamma_H < (15.7\ ^{-2.9}_{+3.9})\ \Gamma_H^{SM}\ \text{at 95\% c.l.}\ .$$

Theoretical improvements

* Because of large scale uncertainty, we need a campaign to calculate the complete gg-initiated contributions at NLO, (Higgs portion is already known).
* Helpful to complete the full NNLO cross section.
* It may be experimentally helpful to separate the data in jet bins: this too will also require further theoretical work to calculate rates in 1-jet, 2-jet..

$pp \rightarrow W^+W^- \rightarrow \nu e^+\mu^-\nu$

WW production in MCFM

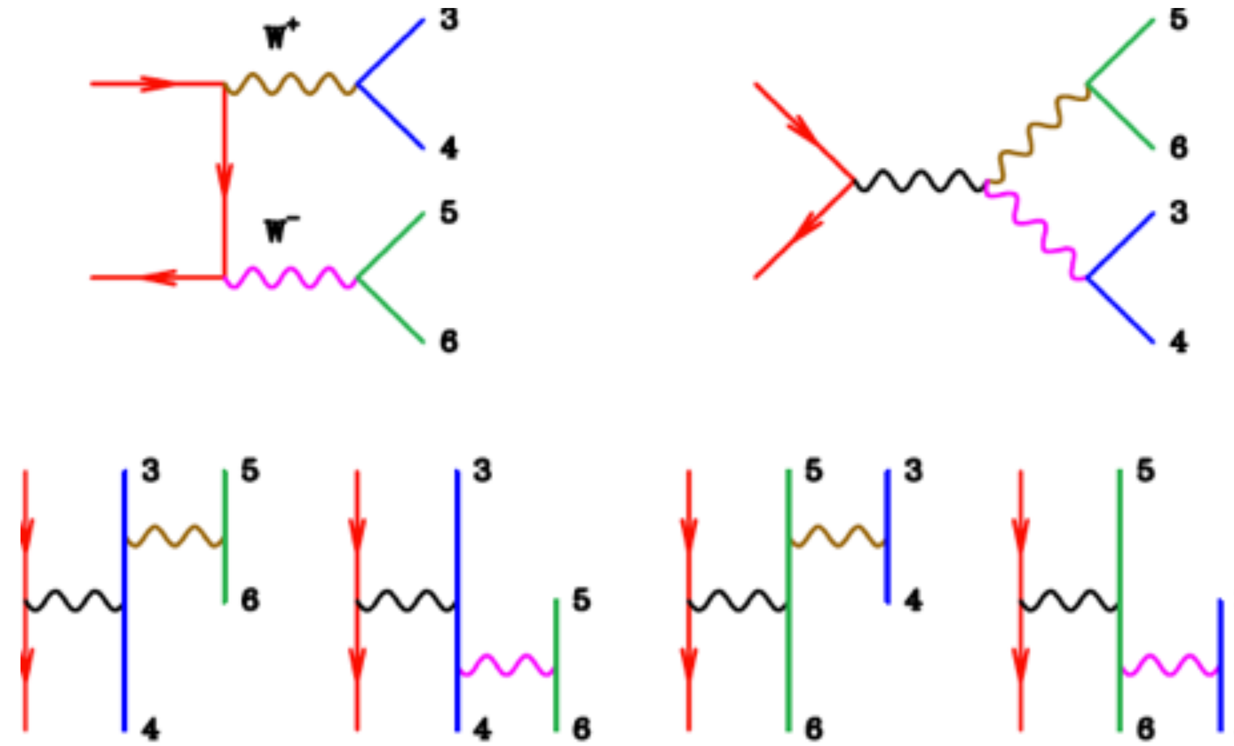

- Includes both doubly resonant and singly resonant diagrams with Z/γ*.
- Full NLO-Virtual corrections from DKS, (hep-ph/9803250)
- Includes gg fermion loop contributions, that are formally higher order, using compact analytic formulae, $m_t \neq 0, m_b = 0$

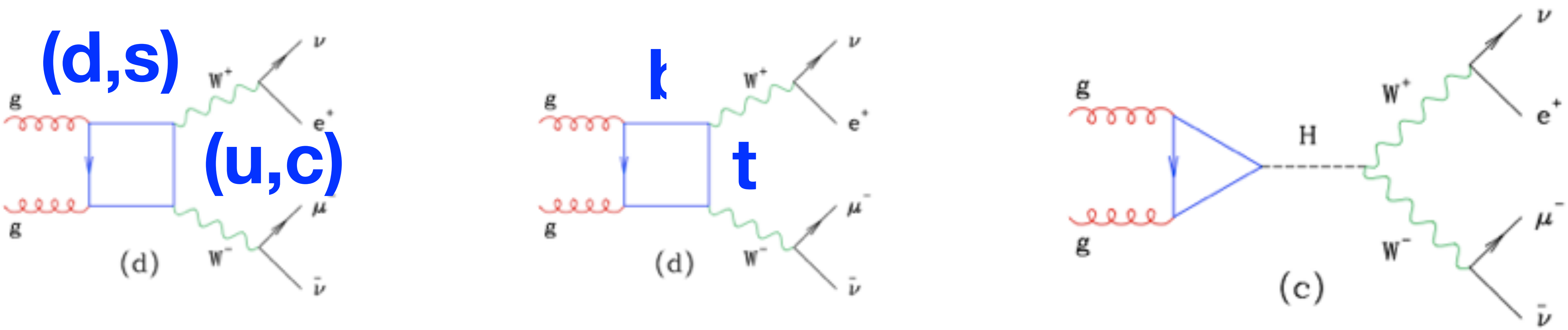

Bounding Γ_H with for $H \to WW$

- WW* channel has advantages over ZZ*.
  - Threshold for real WW production is closer
  - $BR(H \to WW^*) x Br(W \to l\nu)^2 \approx 100\ BR(H \to ZZ^*) x Br(Z \to l^- l^+)^2$
- Disadvantages
  - Larger backgrounds especially top - need jet veto.
  - No 5σ "discovery" of Higgs boson in this channel yet.
  - Mass resolution for m_{4l}?

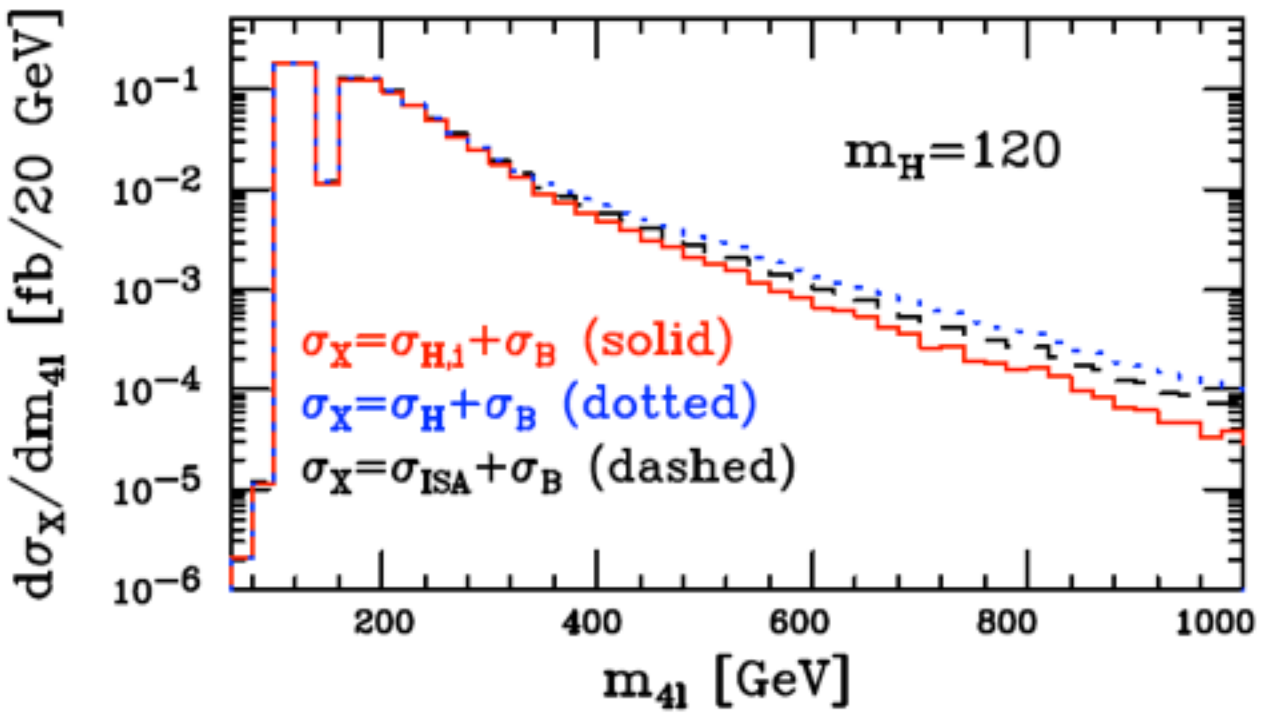

Sizable off-resonant cross section in this channel too.

arXiv1107.5569

Big picture for WW events.

- Follow an ATLAS analysis, ATLAS-CONF-2013-030
- Plotted vs M_T

$$M_T^2 = (E_T^{miss} + E_T^{\ell\ell})^2 - |\mathbf{p}_T^{\ell\ell} + \mathbf{E}_T^{miss}|^2$$

$$E_T^{\ell\ell} = (|\mathbf{p}_T^{\ell\ell}|^2 + m_{\ell\ell}^2)^{1/2}$$

- Analysis targeted at signal peak, not at the resonant tail.
- Edge near Higgs peak clearly visible, but resonant tail strongly suppressed.

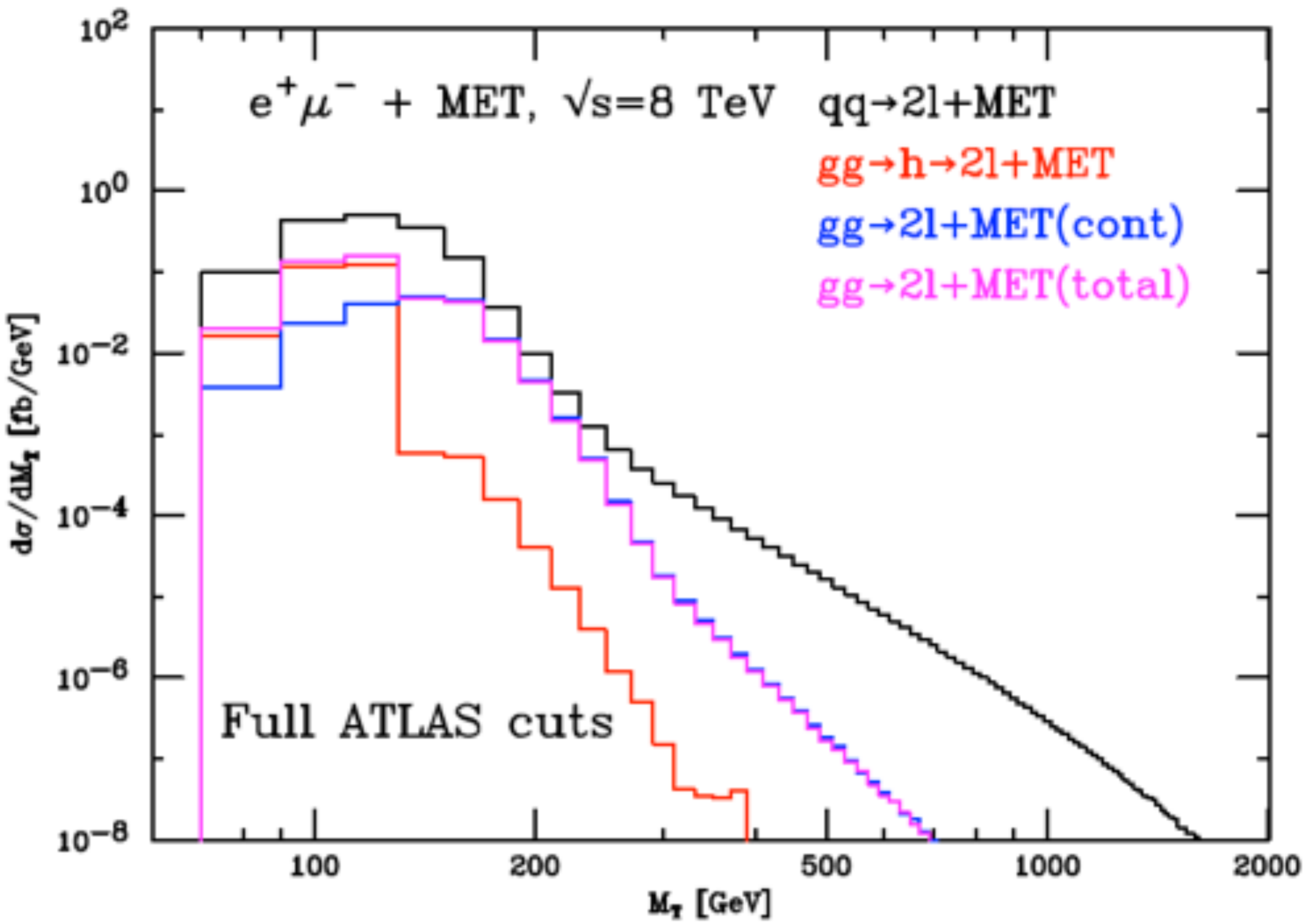

ATLAS "full" cuts

$|\eta_e| < 2.47$ excluding $1.37 < |\eta_e| < 1.52$	
$|\eta_\mu| < 2.5$	$10 \text{ GeV} < m_{\ell\ell} < 50 \text{ GeV}$
$p_T^\ell(\text{hardest}) > 25 \text{ GeV}$	$\Delta\phi_{\ell\ell} < 1.8$
$p_T^\ell(\text{softest}) > 15 \text{ GeV}$	$E_{T,miss}^{rel} > 25 \text{ GeV}$
$p_T^{\ell\ell} > 30 \text{ GeV}$	$|\Delta\phi_{\ell\ell,MET}| > \pi/2$

Big picture with "basic" cuts

* "Basic" cuts = "full" cuts - ($m_{\ell\ell} < 50\,\text{GeV}\,, \quad \Delta\phi_{\ell\ell} < 1.8$)

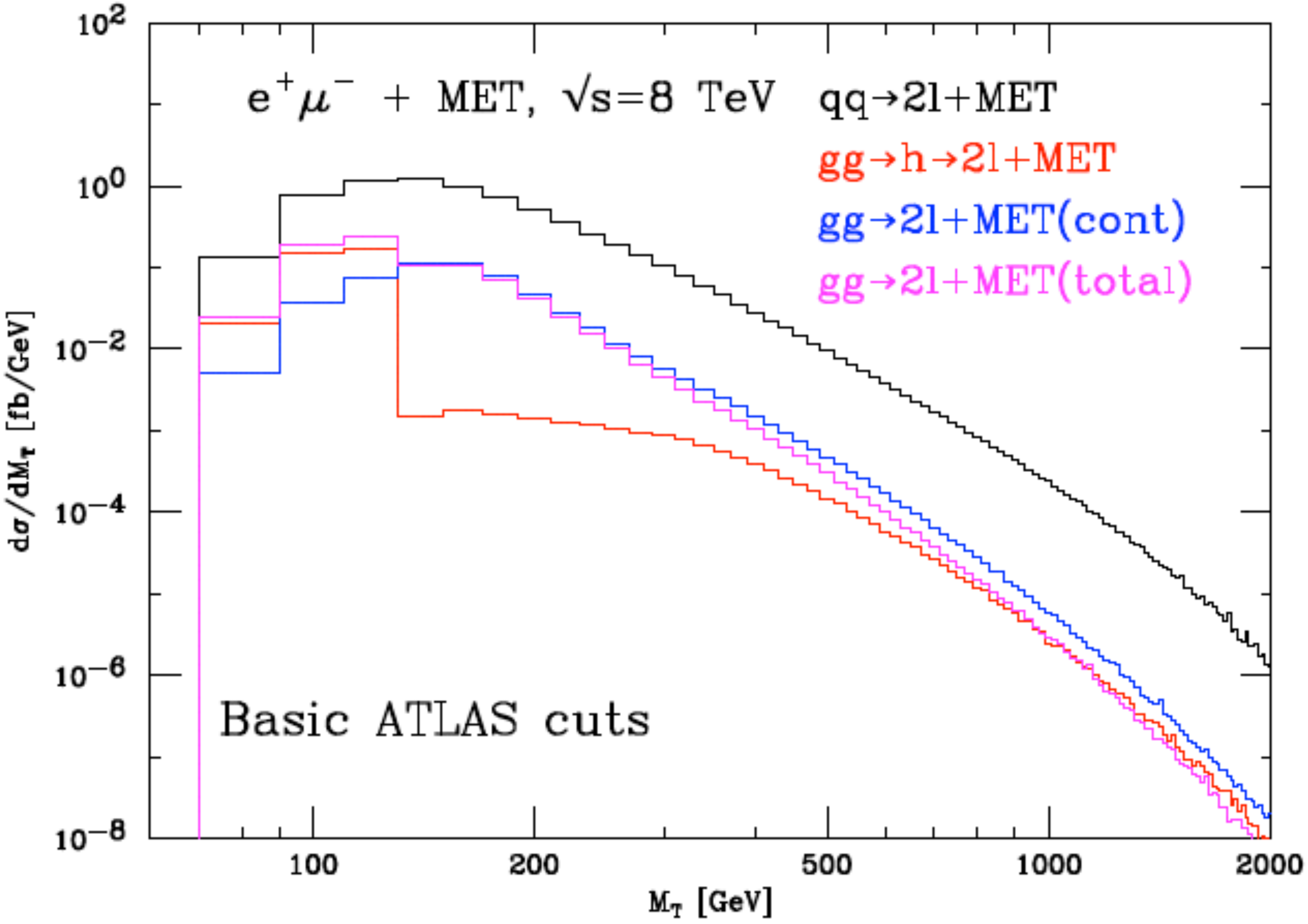

* M_T variable adequate to separate peak and off-peak.

Big picture with basic cuts + $\Delta\Phi_{ll}$ <1.8

* $\Delta\Phi_{ll}$ cut alone provides suppression of continuum background, without strong suppression of gg tail.

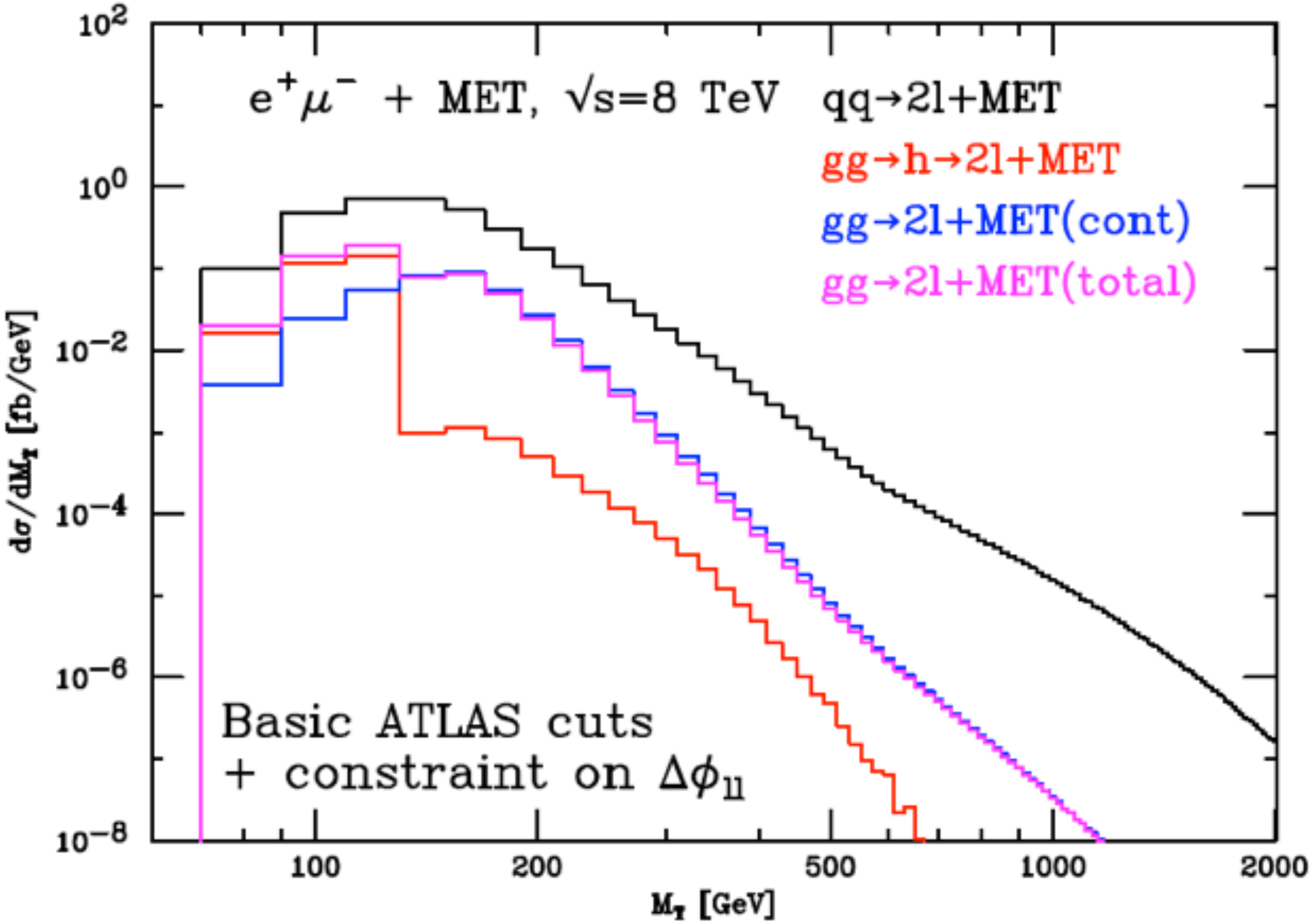

Numbers @ 8 and 13 TeV.

$$\sigma^H : |\mathcal{M}_H|^2, \quad \sigma^I : |\mathcal{M}_H+\mathcal{M}_C|^2-|\mathcal{M}_C|^2-|\mathcal{M}_H|^2$$

Cuts	$M_T < 130$ GeV		$M_T > 130$ GeV		$M_T > 300$ GeV	
	σ^H	σ^I	σ^H	σ^I	σ^H	σ^I
full	5.06	-0.0778	0.0262	-0.173	-	-
basic + $\Delta\phi_{\ell\ell}$	5.52	-0.0924	0.0844	-0.483	0.0021	-0.00888
basic	6.85	-0.117	0.328	-1.07	0.104	-0.240

Cuts	$M_T < 130$ GeV		$M_T > 130$ GeV		$M_T > 300$ GeV	
	σ^H	σ^I	σ^H	σ^I	σ^H	σ^I
full	11.3	-0.195	0.0658	-0.431	-	-0.000185
basic + $\Delta\phi_{\ell\ell}$	12.3	-0.233	0.222	-1.25	0.00698	-0.0283
basic	15.2	-0.296	1.04	-3.15	0.393	-0.893

- Interference is primarily an off-resonant phenomenon.
- Interference relatively more important than for ZZ
- With the basic cuts σ^{peak}(13TeV)≈ 2 σ^{peak}(8TeV) whereas $\sigma^{\text{off-peak}}$(13TeV)≈ 3 $\sigma^{\text{off-peak}}$(8TeV), so method will improve with energy.

“Extraction” of limit from ATLAS data-full cuts

- Using a series of plausible assumptions about errors....
- 7.4% ATLAS error on WW background.

$$\Gamma_H < 365^{+118}_{-79}\, \Gamma_H^{SM}$$

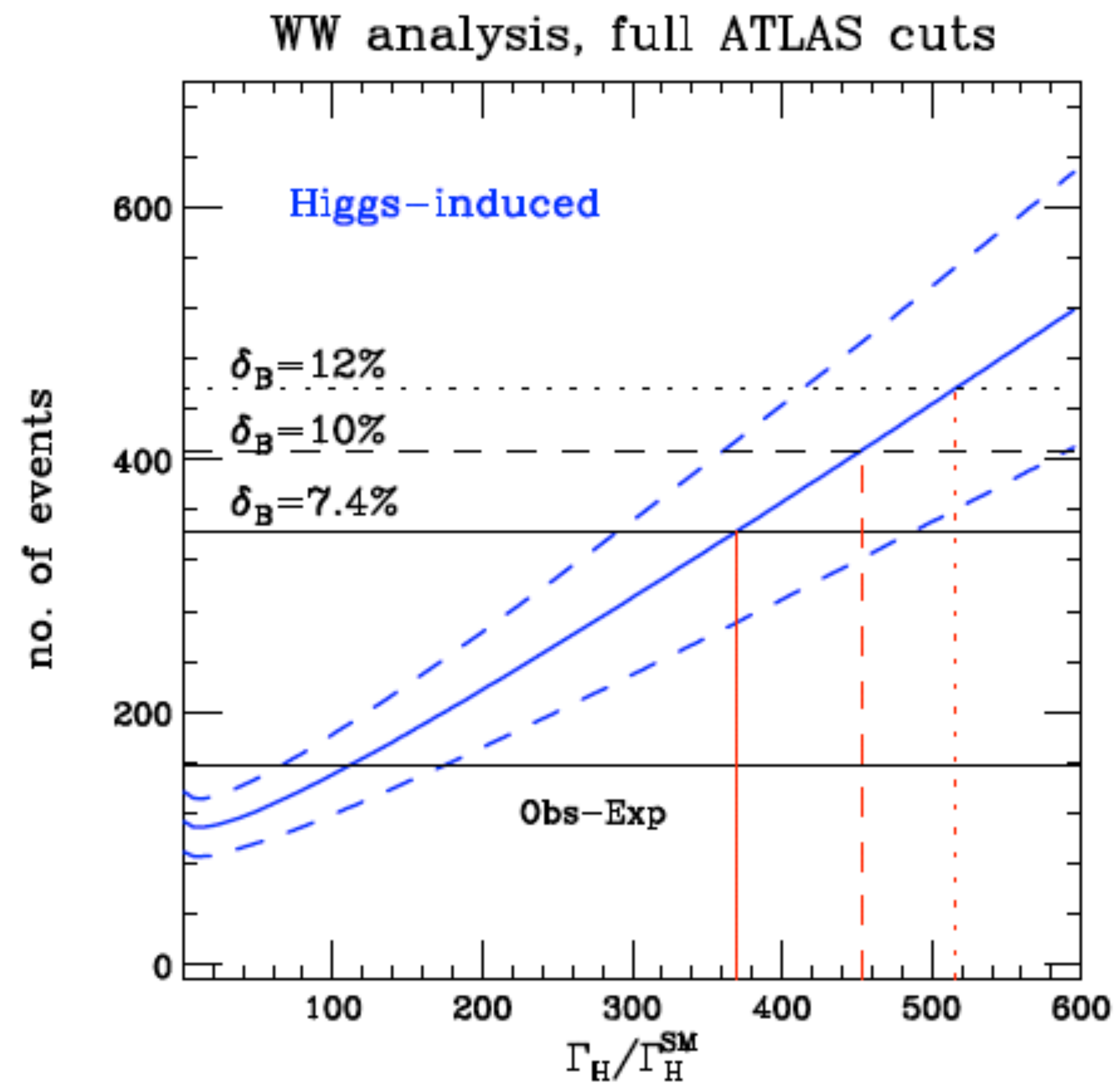

ATLAS data - basic cuts.

$$\Gamma_H \; < \; 125^{+23}_{-22} \, \Gamma_H^{\rm SM}$$

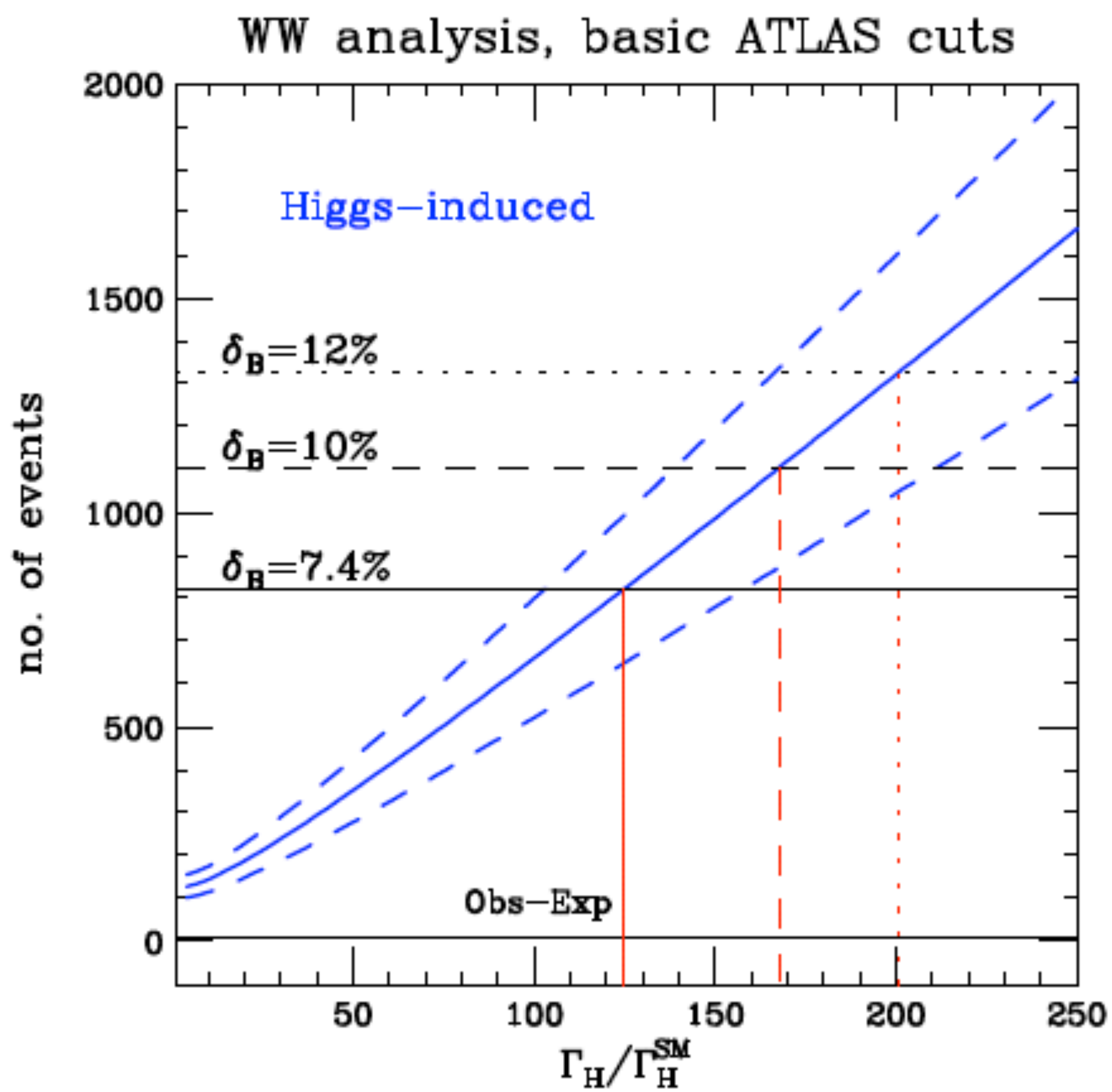

ATLAS data, M_T>300GeV

- For example the expected 95% confidence limit for a 10% background uncertainty

$$\Gamma_H < 45^{+9}_{-7}\,\Gamma_H^{\rm SM}$$

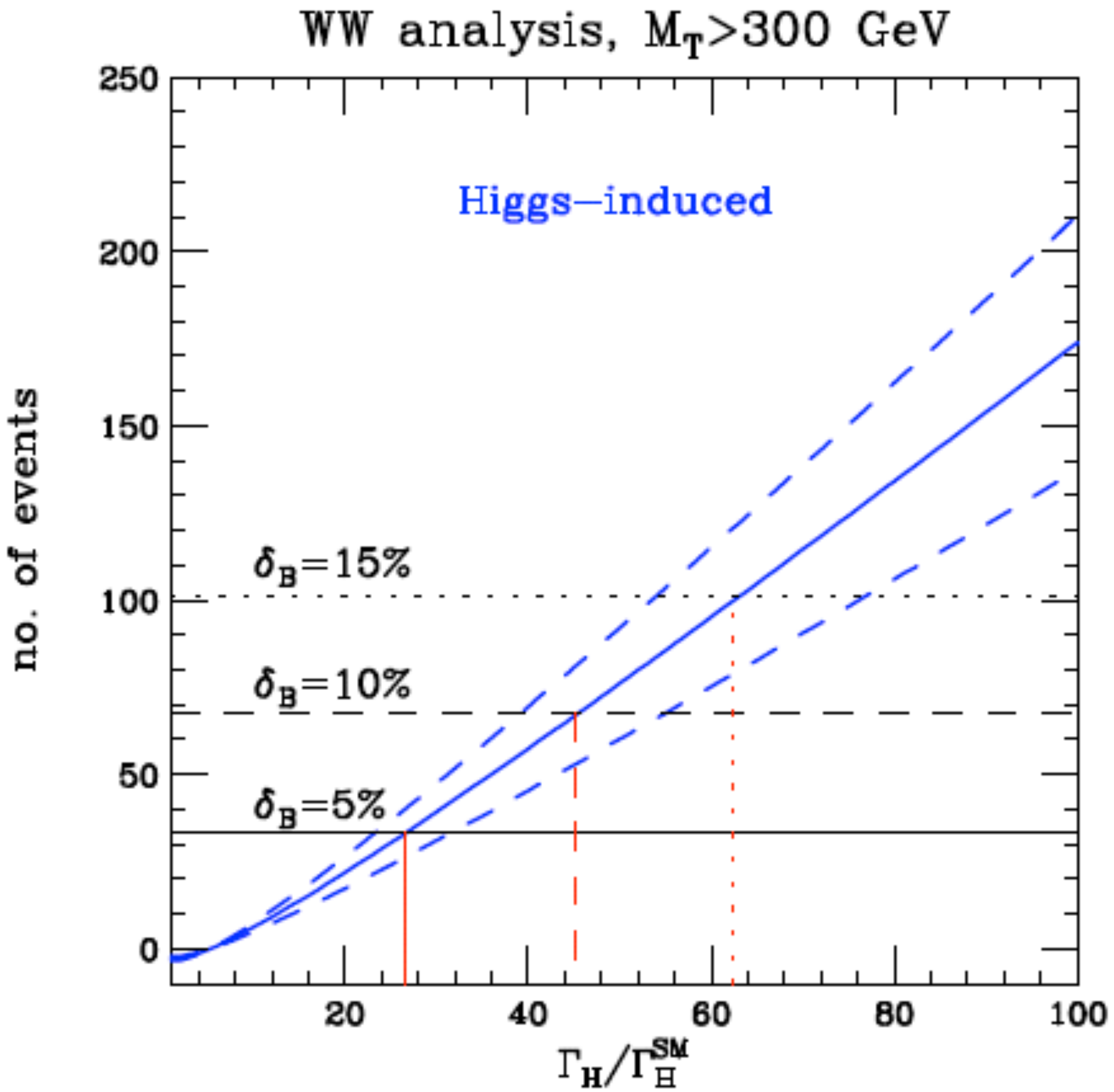

Mass shift due to interference in $H \to \gamma\gamma$.

- S. Martin 1208.1533,1303.3342,De Florian et al 1303.1397, Dixon Li 1305.3854

* Expected inclusive mass shift is of order 70MeV at NLO
* Relies on mass shift due to interference in γγ channel and control channel $ZZ^* \to l^+l^-l^+l^-$
* Experiments do not agree on the sign of this shift.
* ATLAS: $m_h^{\gamma\gamma} - m_h^{ZZ} = +2.3^{+0.6}_{-0.7} \pm 0.7\,\text{GeV}$
* CMS: $m_h^{\gamma\gamma} - m_h^{ZZ} = -0.4 \pm 0.7 \pm 0.6\,\text{GeV}$
* "What we can say is that taking $\Gamma_h = 200\Gamma_{SM} = 800\,\text{MeV}$ would result in a mass shift of order 1GeV, in the same range.." as given above. • Dixon Li 1305.3854

Summary on (potential) current bounds on Higgs width

- Measurement methods,
  - Width convoluted with resolution
  - Mass shift in γγ mode due to interference (c.f Lance Dixon, Edinburgh, Jan2014)
  - Comparison of on-shell-off-shell rate (CM method)
- Other methods involve theoretical assumptions, typically that the Higgs coupling to electroweak vector bosons does not exceed the SM value, (eg. Dobrescu, Lykken, 1210.3342 and CMS PAS HIG-13-005, $\Gamma_H / \Gamma_H^{SM} < 2.8$)

Method	Measured quantity	Γ_H [MeV]	Γ_H/Γ_H^{SM}
CMS-PAS-HIG-13-016	Width $\times$ resolution	< 6900	< 1600
1312.1628 (CEW)	Off-peak/on-peak WW, $m_T > 130, 300$	$< 500 - 180$	$< 125, 45$
1311.3589 (CEW)	Off-peak/on-peak ZZ, $m_{4l} > 130, 300$,MEM	$< 170, 100, 60$	$< 43, 25, 15$
1305.3854(Dixon-Li)	Higgs mass in $\gamma\gamma$,	< 800	< 200

A limit of ~15Γ_{SM} with current data

Summary on future bounds on Higgs width

- Comparison of methods

Method	Measured quantity	Γ_H [MeV]	Γ_H/Γ_H^{SM}
1305.3854(Dixon-Li) 3 ab^{-1}	Higgs mass in $\gamma\gamma, \Delta m_H \sim 100$ MeV	< 60	< 15
1307.4935 (CM) 3 ab^{-1}	Off-peak/on-peak ZZ, $m_{4l} > 130, 300$	$< 40, 20$	$< 10, 5$

- CM method appears to be the winner, at least until the start of lepton collider operation......

Conclusions

* We have re-calculated the continuum background process $gg \to ZZ \to e^- e^+ \mu^- \mu^+$ providing compact analytic formula.
* We have written a fast code that is numerically stable without recourse to multiple precision and is included in MCFM. Released 6-DEC-2013.
* LHE events are available.
* We essentially confirm the results of Caola and Melnikov, although we differ in details, primarily because of choice of scale $m_{4l}/2$.
* The method shows sufficient promise that it merits a concerted effort to calculate (N)NLO/EW corrections to the $Z/\gamma^* Z/\gamma^* \to e^- e^+ \mu^- \mu^+$ process.
* Matrix element method can lead to a further improvements.
* WW process gives important complementary information and should be pursued too.
* So ... the ball is in the experimenter's court now.

Snowmass projections for Higgs coupling measurements

Facility	LHC	HL-LHC	ILC500	ILC500-up	ILC1000	ILC1000-up	CLIC	TLEP (4 IPs)
$\sqrt{s}$ (GeV)	14,000	14,000	250/500	250/500	250/500/1000	250/500/1000	350/1400/3000	240/350
$\int \mathcal{L}dt$ (fb^{-1})	300/expt	3000/expt	250+500	1150+1600	250+500+1000	1150+1600+2500	500+1500+2000	10,000+2600
κ_γ	$5-7\%$	$2-5\%$	8.3%	4.4%	3.8%	2.3%	$-/5.5/<5.5\%$	1.45%
κ_g	$6-8\%$	$3-5\%$	2.0%	1.1%	1.1%	0.67%	3.6/0.79/0.56%	0.79%
κ_W	$4-6\%$	$2-5\%$	0.39%	0.21%	0.21%	0.2%	1.5/0.15/0.11%	0.10%
κ_Z	$4-6\%$	$2-4\%$	0.49%	0.24%	0.50%	0.3%	0.49/0.33/0.24%	0.05%
κ_ℓ	$6-8\%$	$2-5\%$	1.9%	0.98%	1.3%	0.72%	$3.5/1.4/<1.3\%$	0.51%
$\kappa_d = \kappa_b$	$10-13\%$	$4-7\%$	0.93%	0.60%	0.51%	0.4%	1.7/0.32/0.19%	0.39%
$\kappa_u = \kappa_t$	$14-15\%$	$7-10\%$	2.5%	1.3%	1.3%	0.9%	3.1/1.0/0.7%	0.69%

New in MCFM 6.7, (December 2013)

- New analytic implementation of gg→ZZ box contribution including massive loop.
- Unweighted events for $gg \to ZZ^* \to e^- e^+ \mu^- \mu^+$ and $gg \to H \to ZZ^* \to e^- e^+ \mu^- \mu^+$ including interference available in LHE format.
- Added triphoton production at NLO.
- Added double Higgs production at one-loop (LO).
- Improved PDF uncertainty output.
- Fixed treatment of errors in histograms.

Higgs cross sections

- Higgs cross sections in MCFM

Process	Order	Comment
$pp \to H$	NLO	effective theory $m_t \to \infty$
$pp \to H + 1$ jet	NLO	effective theory $m_t \to \infty$
$pp \to H + 2$ jets	NLO	effective theory $m_t \to \infty$
$pp \to H + 2$ jets	NLO	Vector boson fusion W and Z exchange
$pp \to W^\pm H$	NLO	W decay to $l\nu$ included
$pp \to ZH$	NLO	Z-decay to $l\bar{l}$ included
$pp \to t\bar{t}H$	LO	top decay to $bl\nu$ included

- Many of these cross sections are known at NNLO, so MCFM is not state of the art in this regard.
- The most precise theoretical cross sections will be important in the coupling measurement phase.

MCFM

- MCFM is a unified approach to NLO corrections, both to cross sections and differential distributions: http://mcfm.fnal.gov (v6.7, December 6, 2013).
- Publically available code, J. M. Campbell, R. K. Ellis, C. Williams (main authors) R. Frederix, H. Hartanto, F. Maltoni, F. Tramontano, S. Willenbrock, G. Zanderighi....
- Standard Model processes for di-boson pairs, vector boson+jets, heavy quarks, Higgs, photon processes,... (~160 different processes included at NLO).
- Decays of unstable particles are included, maintaining spin correlations.
- Amplitudes (especially the one-loop contributions), calculated *ab initio* or taken from the literature.
- Operates as a resource for tree and NLO matrix elements.